© 2018. Published by The Company of Biologists Ltd | Journal of Cell Science (2018) 131, jcs209270. doi:10.1242/jcs.209270

REVIEW

SPECIAL ISSUE: PLANT CELL BIOLOGY

Green light for quantitative live-cell imaging in plants

Guido Grossmann[1,2,‡], Melanie Krebs[1,‡], Alexis Maizel[1,‡], Yvonne Stahl[3,‡], Joop E. M. Vermeer[4,*,‡] and Thomas Ott[5,§]

ABSTRACT

Plants exhibit an intriguing morphological and physiological plasticity that enables them to thrive in a wide range of environments. To understand the cell biological basis of this unparalleled competence, a number of methodologies have been adapted or developed over the last decades that allow minimal or non-invasive live-cell imaging in the context of tissues. Combined with the ease to generate transgenic reporter lines in specific genetic backgrounds or accessions, we are witnessing a blooming in plant cell biology. However, the imaging of plant cells entails a number of specific challenges, such as high levels of autofluorescence, light scattering that is caused by cell walls and their sensitivity to environmental conditions. Quantitative live-cell imaging in plants therefore requires adapting or developing imaging techniques, as well as mounting and incubation systems, such as micro-fluidics. Here, we discuss some of these obstacles, and review a number of selected state-of-the-art techniques, such as two-photon imaging, light sheet microscopy and variable angle epifluorescence microscopy that allow high performance and minimal invasive live-cell imaging in plants.

KEY WORDS: Imaging, Plant cell biology, Plant growth

Introduction

Since Robert Hooke's observation of the first cells in the 17th century, plants have been of central importance for numerous key discoveries in cell biology. This is exemplified by the cell theory that was originally formulated in 1838 ('Beiträge zur Phytogenesis') by the botanist Matthias Jakob Schleiden, who suggested that every structural element of plants is composed of cells or their products. The same conclusion was reached a year later by the zoologist Theodor Schwann (Mazzarello, 1999). Modern plant cell biology has greatly benefited from genetic and molecular tools that have enabled visualization of dynamic subcellular processes in living plant cells and helped to shed light on the plastic development of plants.

Plants exhibit an outstanding flexibility of adapting their morphology, optimizing their metabolic activity or the timing of developmental programs to fluctuating environmental conditions, such as the initiation of reproductive organs (De Storme and Geelen, 2014). This plasticity depends on intricate sensing and signaling networks that we are only beginning to unravel. Fluorescence-based microscopy has revolutionized various fields of plant biology, such as large-scale organ morphogenesis, Ca^{2+} signaling during sexual reproduction or membrane protein dynamics during pathogen attack (Barbier de Reuille et al., 2015; Fernandez et al., 2010; Shaw and Ehrhardt, 2013). The need to image live plant cells in intact tissues raised the demand for developing novel experimental tools and setups (Shaw and Ehrhardt, 2013). The greatest challenge is the inherent autofluorescence of most plant cells, which is largely caused by the presence of chlorophyll and carotenoids in plastids, as well as by lignin and other phenolic compounds in cell walls (Shaw and Ehrhardt, 2013). This limits high-resolution approaches, such as single-particle tracking or live-cell imaging of plant samples with low fluorescence, and imaging deep within the tissue. Another challenge is to establish growth systems that allow non-invasive, high-quality imaging of intact and growing plant organs, such as roots, or entire plants.

In this Review, we focus on a number of selected techniques and tools that have recently enabled a number of discoveries in plant cell biology (Fig. 1). We first illustrate several of the key challenges that are inherent to live plant imaging, followed by an introduction into how recent technological developments have allowed plant cell biologists to image deep inside tissues for extended time and in defined micro-environments. Finally, we examine state-of-the-art technical solutions and their limitations for imaging and quantifying the distribution of metabolites, proteins or proteins complexes in live plant tissues. Some additional key technologies, such as super-resolution and imaged-based phenotyping have been recently discussed elsewhere (Komis et al., 2015; Rellán-Álvarez et al., 2015; Schubert, 2017), and will not be covered here.

Challenges of imaging plant cells

Differentiated plants cells feature a vacuole that occupies the bulk space of the cell. Consequently, each plant cell behaves like a lens, and this affects light propagation (Berthet and Maizel, 2016). In addition, plants produce a plethora of metabolic compounds that exhibit autofluorescence characteristics upon excitation. This autofluorescence is most often strongest in the blue, but when investigating photosynthetic tissues, it also masks a large proportion of the red spectrum (Jamme et al., 2013). The simplest option, even though it is often not feasible, is to avoid fluorophores with overlapping excitation or emission spectra. However, in modern confocal systems, there are several ways to minimize autofluorescence cross talk. One approach is spectral unmixing – a common feature of modern confocal microscopes – to eliminate the contribution of autofluorescence to a confocal image (see Glossary). Where tunable lasers are available, for example, in systems for two-photon-excitation microscopy (TPEM), it is highly recommended to scan different excitation wavelengths to select the one with the best signal-to-noise ratio (SNR). A more recent development is the use of flexible pulsed lasers together with detectors that have a photon-counting ability (Kodama, 2016). This allows time-resolved fluorescence detection and gating based on the fluorescence

[1]Centre for Organismal Studies (COS), Heidelberg University, Im Neuenheimer Feld 230, 69120 Heidelberg, Germany. [2]Excellence Cluster CellNetworks, Heidelberg University, 69120 Heidelberg, Germany. [3]Institute for Developmental Genetics, Heinrich-Heine University, Universitätsstr. 1, 40225 Düsseldorf, Germany. [4]Laboratory for Cell Biology, Wageningen University, Droevendaalsesteeg 1, 6708 PB Wageningen, The Netherlands. [5]Faculty of Biology, Cell Biology, University of Freiburg, Schänzlestr. 1, 79104 Freiburg, Germany.
*Present address: Department of Plant and Microbial Biology, University of Zürich, Zollikerstrasse 107, 8008 Zürich, Switzerland.
‡These authors contributed equally to this work

§Author for correspondence (Thomas.Ott@biologie.uni-freiburg.de)

T.O., 0000-0002-4494-9811

Journal of Cell Science (2018) 131, jcs209270. doi:10.1242/jcs.209270

Glossary

Abbe–Raleigh criteria: two closely related values for the diffraction limit. Although very similar, the difference between the two is the definition that Abbe and Rayleigh used for what defines two objects being resolvable from each other:

Abbe criterion $d = \frac{0.5\lambda}{NA}$

Rayleigh criterion $r = \frac{0.61\lambda}{NA}$

Here, r is the difference between two objects, λ the excitation wavelength and NA is the numerical aperture of the objective lens.

Adaptive optics: optical components of which properties can be adjusted to correct optical aberrations caused by refractive index mismatches in the optical path of a microscope and within the specimen.

Electron-multiplying charge-coupled devise (EM-CCD): EM-CCD cameras are characterized by high quantum efficiencies (~90%) and are therefore often used for imaging specimens with low light intensities. Incident photons are converted into photoelectrons and trapped within the imaging region cooled detector, before they are transferred to the storage region, where they are further processed without blocking the detector for the next acquisition. The signals are then amplified and further converted into electric impulses before being digitized to generate an image. Whereas classical CCD cameras reached similar quantum efficiencies, EM-CCDs have an improved reduction of electronic read noise.

Fluorescence correlation spectroscopy (FCS): FCS is carried out in a defined measurement volume (mostly a confocal volume), where the intensity fluctuations of a fluorescently labeled molecule are statistically analyzed over time. By using this method, local concentrations, molecular mass, diffusion coefficients, chemical rate constants and photodynamics can be determined.

Fluorescence cross correlation spectroscopy (FCCS): in FCCS measurements, two separately labeled fluorescent molecules are observed in a defined measurement volume (mostly a confocal volume) over time. If the two molecules interact, the intensity fluctuation of their fluorescent signals correlates. This technique provides a highly sensitive measure to investigate protein–protein interactions independent of diffusion.

Pinhole: the pinhole is an adjustable diaphragm that is placed after the objective into the light path. It restricts further passage of out-of-focus light to reach the detectors. This provides the opportunity to acquire light from a 'confocal' plane, where detection and illumination are focused on the same point.

Pulsed lasers: lasers that deliver energy in pulses of specific duration and frequency.

Scanning FCS: in scanning FCS, the defined measurement volume is moved along the sample in a defined way. The collected data are combined and provide means to overcome challenging conditions for pure FCS measurements, e.g. slow moving molecules, distortions of the measurement volume, photobleaching etc. that are often found in cellular systems.

Scientific complementary metal oxide semiconductor (sCMOS): In contrast to CCD cameras, each pixel is individually amplified in sCMOS cameras which results in fast frame readouts of up to 5.5 megapixels at 30 frames/s and low electronic read noise. Modern sCMOS sensors reach quantum efficiencies of ~95%.

Spectral unmixing: this approach uses spectral detectors that can record emission spectra of fluorescent probes. These spectral fingerprints can be used to detect multiple fluorescent probes, even with overlapping, but different emission spectra.

Tunable lasers: lasers in which the output wavelength can be adjusted over a wide range of values, which allows the precise excitation of fluorophores.

Widefield microscopy: a microscopy setup where the sample is illuminated from above (upright systems) or below (inverted systems) and the entire two-dimensional image is acquired simultaneously using a wide-area detector, such as a camera. Epifluorescence refers to the widefield detection of fluorescent light, whereas for white light, one refers to brightfield.

lifetime of the respective molecule(s). As autofluorescence typically has a very short lifetime (picosecond range), selecting for the longer lifetimes of fluorescent proteins (nanosecond range) can eliminate a large proportion of the autofluorescence (Kodama, 2016). Besides advances on the instrumentation side, clearing techniques that diminishes chlorophyll autofluorescence while maintaining fluorescent protein stability, such as CLEARSEE (Kurihara et al., 2015), have facilitated imaging-based approaches. Although these protocols are not compatible with living tissue, they can be extremely useful to improve imaging of thick specimens or tissues that normally exhibit strong autofluorescence.

In addition, tropic responses to light and gravity have to be considered in plants. With a few exceptions (see light sheet microscopy below), conventional microscopes are built to hold specimens on horizontal stages. This horizontal mounting, however, conflicts with plant gravitropism, which leads to shoots bending up, and roots bending downwards (Muday, 2001). To allow vertical mounting, a recent study presented a custom-made tilted confocal laser-scanning microscope that does not constrain the gravitropic response of the plant (von Wangenheim et al., 2017). This combined hardware and software solution enables tracking of the root tip while it grows along the gravity vector, and therefore opens up new avenues for studying undisturbed root growth with cellular resolution (von Wangenheim et al., 2017). However, this solution relies on the customization of a microscope, which may limit its widespread adoption in the community. In summary, although live imaging of plants poses specific challenges (autofluorescence and the natural tropic responses of plants), technical solutions have been found to diminish these and allowed for the emergence of specific imaging techniques (Table 1).

Imaging in a controlled micro-environment – the use of microfluidics

Over the past years, several techniques have been developed that enable non-invasive imaging of roots down to the cellular level. Specific imaging setups allow growth of plants either between cover glass and a mesh separating roots from soil (Froelich et al., 2011), on sterile medium with roots being covered with gas-permeable, transparent plastic film (Fournier et al., 2008), or imaging and perfusion of seedlings within self-made chambers (Kirchhelle and Moore, 2017; Krebs et al., 2012). One milestone was the development of microchannel platforms for *Arabidopsis* roots (Grossmann et al., 2011; Meier et al., 2010; Parashar and Pandey, 2011) that took advantage of the compact design, versatility and cost-effective fabrication of polydimethylsiloxane (PDMS)-based microfluidic devices. Here, primary roots grow into observation chambers; thereby, specimen mounting occurs without direct specimen handling. The possibility to cultivate roots in protected chambers inside devices that match the needs that are specific to the experiment has substantially facilitated quantitative and dynamic measurements and provided the ability to precisely control the plant microenvironment. Lab-on-a-chip devices are typically characterized by miniature channel systems that guide the flow of

Journal of Cell Science (2018) 131, jcs209270. doi:10.1242/jcs.209270

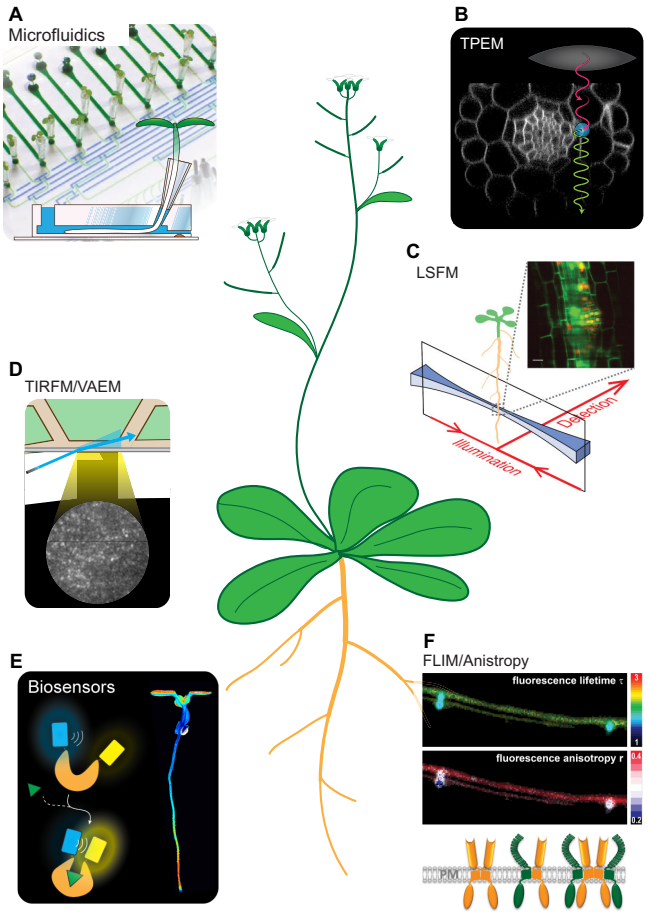

Fig. 1. Imaging techniques for next generation plant cell biology. (A) Microfluidics. Integrated plant-on-chip devices have significantly improved experimental access in particular to root development, physiology and signaling. They allow long-term measurements on growing organs under precisely controlled conditions. The technique takes advantage of seedlings growing into perfusion chambers (blue cavity), thus allowing precise control over the root microenvironment. (B) TPEM. Two-photon excitation microscopy has enabled deep-tissue imaging by evading the light-scattering effects of plant cell walls. To generate high-resolution *z*-sections (the background image shows a cross-section of an *Arabidopsis* root), this technique is based on two low-energy photons (red) being combined in the focal plane (blue spot) to excite the target fluorophore (emission shown in green). (C) LSFM. Light sheet fluorescence microscopy has substantially advanced rapid whole organ time-lapse imaging, thereby reducing phototoxicity and keeping photobleaching to a minimum. For LSFM, the specimen is illuminated with a thin sheet of excitation light, perpendicular to the detection path. (D) TIRF microscopy and/or VAEM. Variable-angle epifluorescence microscopy has allowed plant scientists to benefit from the improved contrast and sensitivity that are typical features of total internal reflection fluorescence microscopy, despite the thick cell wall that usually prevents TIRF microscopy to be applied to plant cells. In contrast to TIRF, the parts of the specimen that are close to the cover glass are illuminated with an inclined laser beam. Varying the illumination angle allows to adjust the light penetration depth. (E) Biosensors. Genetically encoded fluorescence-based sensors for small molecules have enabled the dynamic imaging of metabolites and signaling molecules. Readouts such as signal intensity or FRET (as depicted on the left) allow quantitative measurements of small molecules on the subcellular or organismal level. Right, a heat-map showing steady-state levels of cytosolic calcium throughout an *Arabidopsis* seedling. (F) FLIM and/or anisotropy. Fluorescence lifetime imaging, combined with fluorescence anisotropy measurements, has recently been established for the *in vivo* detection of protein–protein interactions and protein complex composition.

Table 1. Challenges and solutions for live-cell imaging application in plants

Challenges	Solutions
Autofluorescence from chlorophyll, carotenoids and phenolic compounds limit single-particle tracking, imaging of samples with low fluorescence and deep-tissue imaging	Spectral-based unmixing, lifetime-based unmixing and application of clearing techniques (not compatible with live imaging) can be used to avoid autofluorescence from plant tissues
Light scattering that is caused by cell walls and air-spaced tissues limits imaging of samples with low fluorescence and deep-tissue imaging	Application of clearing techniques and vacuum infiltration can be used to reduce light scattering in plant tissues
Image plants in a minimal-invasive way under near-physiological conditions	Application of vertical stage microscopy, custom-built perfusion chambers and microfluidic devices to guarantee a stable plant microenvironment for prolonged periods of time
Cell wall impregnations such as cutical waxes or suberin depositions limit the uptake of substances during live-cell imaging	Cell wall digestion, preparation of epidermal strips or tissue infiltration can be used to overcome this physical barrier
Localized applications of treatments	Application of micromanipulators, laminar-flow techniques, micro-beads and OEIPs can be used for local stimulus application
Silencing of GEFIs	Use of alternative promoters that are less prone to silencing and expression in silencing-deficient mutant background provide strategies to overcome GEFI silencing

liquids and enable parallel and multiplexed analyses, while consuming minimal fluid volumes (Sia and Whitesides, 2003). Although cell biologists have already utilized microfluidic devices for some time to allow long-term cultivation of microbes or eukaryotic cell cultures (Whitesides, 2006), this technology has found its way into organismal biology only more recently and is now applied to multicellular organisms, such as nematodes, insects, fish and mammalian embryos and plants (Stanley et al., 2016). The adoption of the microfluidic lab-on-a-chip technology for plant cell biology has enabled novel approaches to explore environmental sensing, cellular and organ growth mechanics, and nutrient uptake kinetics.

As an example, the *RootChip* (Fig. 2A) was developed to host growing primary roots of *Arabidopsis* seedlings that can be subjected to pulsed treatments (Grossmann et al., 2011). Often used in combination with genetically encoded fluorescent sensors (see below), the *RootChip* technique has been applied to various imaging-based applications. Examples are quantitative analyses of small-molecule dynamics during nutrient transport (Grossmann et al., 2011), heavy-metal homeostasis (Lanquar et al., 2014), hormone (Jones et al., 2014) and Ca^{2+} signaling (Denninger et al., 2014; Keinath et al., 2015), as well as quantitative root phenotyping (Grossmann et al., 2012; Xing et al., 2017). As a high-throughput root-observation platform, the *RootArray* has enabled quantitative analyses of cell fate-specific gene expression of 64 roots in parallel (Busch et al., 2012). To facilitate high-resolution phenotyping of even larger numbers of *Arabidopsis* seedlings, a microfluidic device with automatic trapping of seeds in micro-wells has been developed (Jiang et al., 2014).

Journal of Cell Science (2018) 131, jcs209270. doi:10.1242/jcs.209270

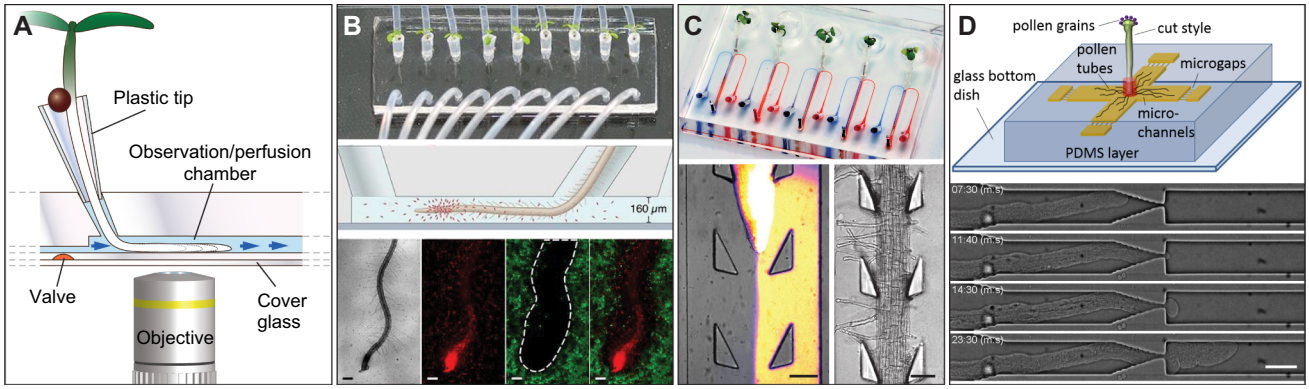

Fig. 2. Microfluidic tools for environmental control during live-imaging of roots and pollen tubes. (A) *RootChip* principle. *Arabidopsis* seeds are germinated on plastic tips and roots grow into an observation chamber, where the root tip is subjected to liquid flow and becomes accessible for imaging. An optional valving system provides precise control over the flow during experiments where conditions need to be changed rapidly. Imaging typically occurs on an inverted microscope. Schematic adapted with permission from Grossmann et al. (2011). (B) The tracking root interactions system (TRIS) platform is used to perfuse growing roots with fluorescent bacteria, which reveals competition in colonizing roots between *Bacillus subtilis* (red fluorescence, bottom panels) and *Escherichia coli* (green fluorescence). Scale bars: 200 µm. Images reproduced with permission from Massalha et al., 2017. (C) The dual-flow-*RootChip* enables asymmetric treatments of individual roots. By utilizing laminar flow along the root axis, two different microenvironments can be generated, which was used to unveil local adaption of root development and physiology. Scale bars: 100 µm. Images used with permission from Stanley et al., 2017. (D) Example of a device for probing the capability of tip-growing plant cells, here pollen tubes, to penetrate narrow gaps. Scale bar: 20 µm. Schematic and time series reproduced with permission from Yanagisawa et al., 2017.

A benefit of long-term cultivation of live specimens in microfluidic perfusion systems is their potential to aid studies on interorganismic interactions: one of the earliest devices was designed to observe the feeding of nematodes on *Arabidopsis* roots, as well as the infection of roots with bacterial plant pathogens (Parashar and Pandey, 2011). Recent work has expanded this approach to investigate the formation of microbial biofilms along specific root zones (Massalha et al., 2017) (Fig. 2B). These examples highlight the possibilities of microfluidic devices to open up new avenues to gain a better understanding of plant development in complex biological environments (Stanley et al., 2016). Microfluidic devices will therefore likely push the boundaries of research on plant–microbial communities (Stanley and van der Heijden, 2017).

A technical challenge in any perfusion system is the targeted application of treatments to selected regions of the specimen. In all the microfluidic systems that are mentioned above, plant organs are subject to global treatments. However, environmental conditions are often highly heterogeneous, with local differences in nutrient availability, the chemical milieu or microbial abundance. Cellular Ca^{2+} responses have been recorded in experiments using micromanipulators to apply localized force to single epidermal cells in roots (Monshausen et al., 2009). A first approach to apply a local stream of liquid within a microfluidic device with a resolution close to that of a micromanipulator probe was developed by the use of a focused laminar flow that was directed perpendicular to a mounted *Arabidopsis* root (Meier et al., 2010). Here, the localized treatment with the phytohormone auxin resulted in arrested cell elongation and root hair development at the site of stimulation (Meier et al., 2010). Such a local application to roots had previously been approached by the application of auxin-loaded sephadex beads along the root, which led to the finding that auxin gradients play a role in planar polarity, defining the regular positioning of root hairs in the root epidermis (Fischer et al., 2006). Recently, the accurate positioning of external auxin gradients was achieved by employing organic electron ion pumps (OEIPs), which can deliver charged compounds at high spatial resolution to roots grown on gelled media (Poxson et al., 2017). In addition, a novel adaptation of the *RootChip* concept now allows the generation of asymmetric root environments by guiding root growth through a micropillar array and perfusing the root with different liquids on either side (Stanley et al., 2017) (Fig. 2C). This approach enables the simulation of environmental heterogeneity and the investigation of cell autonomous and systemic mechanisms of root development.

Microfluidic devices have also substantially advanced experimental access to other plant systems. The moss *Physcomitrella patens*, an emerging model to study plant evolution, features a filamentous network of tissues that makes long-term imaging of growth and development challenging when conventional mounting techniques are being used (Bascom et al., 2016). The first microfluidic device for moss solved this issue by guiding growing filaments through an intermittent barrier into an observation chamber, where they can be studied outside the dense protonemal meshwork (Bascom et al., 2016). For another tip-growing plant cell type, pollen tubes, several micro-devices have already been developed to investigate diverse cellular properties, such as their growth dynamics (Nezhad et al., 2013), their chemo-attraction by the female gametophyte (Horade et al., 2013) and their ability to penetrate narrow gaps (Yanagisawa et al., 2017) (Fig. 2D).

Taken together, microfluidic devices have substantially improved access for imaging plant tissues at high resolution and over extended periods of time. The application of microfluidics will, for some time, remain limited to young seedlings or isolated parts of plants. However, owing to their design flexibility, microfluidic devices bear great potential for cell biological studies in combination with new imaging techniques that require non-invasive specimen immobilization, environmental control and time-lapse imaging with observation times of several days.

Deep imaging of plants through TPEM

Although the combination of advanced growth systems and conventional confocal microscopy has revealed many new biological insights, it is less suited to imaging of deep-lying tissues and thick specimens. Owing to substantial advances in instrumentation and user-friendliness, multi-photon microscopy has become a powerful technique to visualize plant development in 3D.

The most easily implemented and used excitation mode for multi-photon microscopy is the above-mentioned TPEM. Here, two low-

energy (longer, red-shifted wavelength) photons combine in the focal plane to excite the target fluorophore. TPEM makes use of red-shifted wavelengths for excitation without changing the emission spectra. Since the two photons only come together in the focal plane, the energy level that provides excitation is only sufficient in the focal plane. This also reduces photobleaching of regions of the sample that are out of focus, which is an issue in confocal microscopy. As all emitted fluorescence originates from a single focal plane, there is no need for a pinhole (Brakenhoff et al., 1996; Denk et al., 1990; Feijo and Moreno, 2004). Hence, the detectors in a TPEM system can be placed in close proximity to the objective in order to reduce the light path of the emitted fluorescence (i.e. the fluorescence does not pass the scan box again, as is the case when using internal detectors). These 'non-descanned' detectors are required to maintain the full potential of TPEM and are therefore strongly recommended (Ustione and Piston, 2011). Two-photon excitation spectra of fluorescent proteins often differ (slightly) from the one-photon excitation spectra; a property that can be useful to enable simultaneous imaging of two or more fluorescent proteins with a different single excitation wavelength (Drobizhev et al., 2011, 2009). This accelerates image acquisition and hence reduces phototoxicity. Theoretically, by applying the Abbe–Raleigh criteria (see Glossary), the use of short wavelengths in a well-aligned confocal microscope is half of the resolution of a TPE microscope. However, the strong increase in SNR of TPEM provides a spatial resolution that is very similar to that of standard confocal microscopes (Ustione and Piston, 2011).

In addition to these technical developments, the availability of a large set of cell type-specific promoters in *Arabidopsis thaliana* has been instrumental to improve imaging of deep-lying tissues (Birnbaum et al., 2003; Gooh et al., 2015). The expression of a fluorescent protein fusion in the tissue of interest makes it more straightforward to interpret generated images, as no signal that can obstruct the view is derived from surrounding tissues. Recently, the combined use of cell type-specific promoters and TPEM has been used to perform, for the first time, live-cell imaging and cell lineage tracing in developing *Arabidopsis* embryos with unprecedented temporal and spatial resolution (Gooh et al., 2015). Moreover, a related study from the same group revealed the differential contributions of the microtubule and actin cytoskeleton during the first asymmetric division in the *Arabidopsis* zygote. By comparing confocal microcopy to TPEM, they clearly showed that the latter resulted in better images (Kimata et al., 2016). One potential drawback of TPEM is the use of high-power lasers for excitation. Therefore, users need to take care to not overheat the samples. However, this feature can be turned into an advantage by using the high-energy TPE microscope to specifically ablate deep-lying cells without disturbing the surrounding cells. The suitability of such an approach was recently shown, when TPEM was applied to specifically ablate single cells in the *Arabidopsis* embryo (Gooh et al., 2015).

In addition, a very recent exciting development is the use of adaptive optics in TPEM, which resulted in a significant increase in resolution; however, this technique has not yet been used on plant specimens (Zheng et al., 2017). Overall, when the goal is deep-tissue imaging with reduced photobleaching, TPEM is clearly the best approach. However, when imaging cell layers at surface or cell cultures, conventional confocal microscopy will be more suited.

Light sheet microscopy for time-resolved imaging of whole organs

The holy grail for many cell and developmental biologists is the ability to capture and analyze cell dynamics within the tissues of an intact organism. Such high-resolution imaging in 3D, deep in tissues, over prolonged periods of time that can range from minutes to hours or days, has already been achieved (De Rybel et al., 2010; Goh et al., 2016); however, maintaining the specimen in physiological conditions currently represents a major challenge. Over the last 10 years, light sheet fluorescence microscopy (LSFM) has emerged as a powerful technology to tackle this challenge (Höckendorf et al., 2012). LSFM differs from traditional fluorescence microscopy in that two optical axes are used. The first axis solely takes care of the illumination of the sample; it collimates a sheet of laser light that is a few micrometers thick. Thereby, it only excites fluorophores that are located in a small volume of the specimen, whereas the rest is kept in the dark. Photons that are emitted in this volume are collected by the second optical axis, which is orthogonal to the illumination axis. This detection axis captures the whole field of view with a camera, without the need of scanning, as it is the case in laser-scanning confocal microscopy. This massive parallelization of detection allows for fast imaging (~20–30 frames per second), thus reducing the duration of exposure of the specimen and the risk of photobleaching and phototoxic effects. In addition, the quantum yield of modern electron-multiplying charge-coupled device (EM-CCD) cameras allows the use of less incoming laser energy to obtain the same SNR, which contributes further to minimize the deleterious effects of exposing the specimen to intense laser light for a long time (Stelzer, 2015) (see Glossary). Beyond this, the major advantage of LSFM becomes evident when one considers the amount of energy that is encountered by the entire specimen when it is imaged iteratively to generate a *z*-stack. In LSFM, individual optical planes are consecutively illuminated, whereas standard confocal microscopes rely on whole-specimen illumination and subsequent elimination of out-of-focus light by using a pinhole in front of the detector. Consequently, and in contrast to LSFM, the amount of energy that is received by the sample in confocal microscopy is proportional to the number of images in the stack. Thus, phototoxic effects are drastically minimized in LSFM (Stelzer, 2015). Despite these clear advantages, LSFM is not perfect. The most notable problem is the scattering of both excitation and emission light, especially for thick specimens. Modern LSFMs combine several technological improvements to minimize these adverse effects of scattering (de Medeiros et al., 2015; Krzic et al., 2012). They are designed around four orthogonal optical axes – two for detection and two for illumination – which allows the simultaneous acquisition of four images and their merging into a single one. In addition, modern LSFMs implement a slit detection mode to minimize the detection of scattered light by the camera: a scanned Gaussian beam is used to generate the light sheet and is synchronized with the rolling shutter camera. With this, only photons that originate from the sharpest area of the image reach the camera (de Medeiros et al., 2015). This feature is reminiscent of the pinhole of a confocal microscope, but with a much-reduced penalty on imaging speed. Of particular importance for long-term imaging (hours to days) is to keep the plant in a close-to-physiological environment. Since its implementation for *Arabidopsis* imaging (Maizel et al., 2011), efforts have focused on emulating the conditions that plants usually encounter in a laboratory set up into the sample chamber of the microscope. Most LSFMs have a design where the sample is held vertically, which is an advantage over most other setups that impose plants to grow horizontally against their natural tropisms. Furthermore, the presence of a light source that emulates the day and night cycle contributes significantly to the survival of the plant during long-term imaging; this guarantees that any observations made have a physiological relevance.

The application of LSFM to plant cell and developmental biology has essentially been focused on the root of *Arabidopsis thaliana* because of its small diameter and good optical properties. The growth dynamics of the primary roots (de Luis Balaguer et al., 2016; Maizel et al., 2011; Sena et al., 2011) and of lateral roots (Lucas et al., 2013; von Wangenheim et al., 2016) have been documented over the course of hours to days at cellular resolution, which revealed new insights on the dynamics of these processes. At the subcellular levels, LSFM has been used to observe the dynamics of the secretory machinery (Berson et al., 2014) and Ca^{2+} dynamics (Costa et al., 2013).

Imaging individual protein complexes using TIRF microscopy

High-resolution imaging of membrane- or sub-membrane-resident proteins or metabolites is often restricted by the limited resolution of confocal systems along the *z*-axis, which results in comparably high SNRs. A potent method to overcome these limitations is total internal reflection (TIRF) microscopy. Different to confocal and epifluorescence microscopes, the angle of the laser beam here is adjusted to a super-critical angle (65–67°), where all light is reflected at the coverslip. This generates an evanescent wave that penetrates the sample for less than 400 nm (Konopka and Bednarek, 2008). Even though this penetration depth is far more than the 6 nm thickness of a plasma membrane, TIRF microscopy provides a viable method to greatly improve the SNR of such samples to discriminate (sub-)membrane protein populations and to perform single-particle tracking (Wang et al., 2015b). Best results are obtained when using a number of specifications that have been adapted to the requirements of imaging plant tissues (Jaqaman et al., 2008; Wang et al., 2015b). When applying TIRF microscopy on plant cells, the existence of the cell wall with its thickness between 0.1–1 µm needs to be considered. As a consequence, and in contrast to cell cultures or fresh protoplast preparations, plant cell plasma membranes are never in direct contact with the coverslip when imaged in a multi-cellular tissue context. This may be seen as an inherent advantage, as it further reduces signals that derive from the deeper cytoplasm, but it is equally a limitation with respect to sample preparation. In contrast to cell wall-free cultured mammalian cells, which can be grown directly on the coverslip, or cell wall-containing unicellular organisms such as yeast, which sediment on the glass, the surface of intact plant tissues is comparably uneven (Koch et al., 2008). As a consequence, most regions will be out of focus and thus dramatically limit the field of view during TIRF image acquisition. This is even further pronounced when imaging intact tissues rather than cultured cells, as specimen thickness and shape result in major regions of the tissue being impossible to image simultaneously. In these cases, and in order to avoid lateral drift of the samples that could be caused by evaporation of the immersion medium from the edges of the coverslip, researchers are well advised to seal their samples prior to image acquisition. The comparably great distance from the cover glass can be partially compensated for by applying limited forces on the specimen to gently lower the plant tissue towards the incident light beam (Wan et al., 2011). To further overcome the limitation of distance from the cover glass, variable angle epifluorescence microscopy (VAEM) has been introduced for plant cell imaging (Konopka and Bednarek, 2008) and further plant-specific adaptations in laboratory protocols have been evaluated (Wan et al., 2011). In VAEM, sub-critical angles (59–61°) are used for the incident beam that result in the refraction of the light and a narrow field of illumination.

In plants, VAEM and/or TIRF microscopy have been used, among other approaches, for the imaging of the segregation of proteins into plasma membrane nanodomains (Bücherl et al., 2017; Gronnier et al., 2017; Hao et al., 2014; Hutten et al., 2017; Jarsch et al., 2014; Li et al., 2012). In addition, VAEM was used for single-particle tracking of low-abundant receptors such as BRASSINOSTERIOD INSENSITIVE 1 (BRI1), which was found to segregate into two distinct subpopulations of membrane nanodomains with different motion ranges (Wang et al., 2015a) and to interact in discrete nanodomains with its co-receptor (Hutten et al., 2017). Such observations are clearly facilitated by the fact that most TIRF systems use EM-CCD or sCMOS cameras (see Glossary), which have significantly higher quantum yields in comparison to other detectors, such as photo-multipliers (Shaw and Ehrhardt, 2013), as mentioned above. However, a key restriction that applies to TIRF microscopy – as to any other widefield or standard confocal technique – is the resolution limit along the *xy* axis. Although a new class of detector (Huff, 2015) or refined deconvolution approaches (Borlinghaus and Kappel, 2016) allow lateral resolution of structures in the range of ∼140 nm, other approaches are required to precisely described closely associated protein assemblies of physical protein–protein interactions.

In summary, VAEM and/or TIRFM is applicable in plants despite the presence of a plant cell wall. Considering the dimensions of a plant cell, the use of VAEM or TIRFM allows a significant reduction in background fluorescence when imaging membrane-resident and objective-facing proteins, even though the field of view is limited compared to confocal or widefield setups.

In situ measurements using fluorescent indicators

In order to investigate physiological adaptations and dynamics of plant cells on a molecular level, fluorescent indicators are powerful tools that enable non-invasive measurements of various biochemical and biophysical cellular parameters with high spatio-temporal resolution (Table 2). Based on their make-up, small-molecule dye-based fluorescent indicators are distinct from genetically encoded indicators that are based on contain fluorescent proteins and peptides as structural elements. To date, a great variety of fluorescent indicators exist that cover a broad spectrum of applications from the detection of numerous kinds of ions and metabolites to the assessment of cellular redox state, hydrostatic pressure, molecular crowding and membrane potential (Germond et al., 2016; Sanford and Palmer, 2017; Ueno and Nagano, 2011; Uslu and Grossmann, 2016).

Derivatives of small-molecule fluorescent indicators (SMFIs) that permeate the membrane can be easily loaded into cells. However, owing to impregnations of the plant cell wall, such as cuticle waxes or suberin depositions, the loading of SMFIs into intact plant cells is restricted to non-cutinized and non-suberized tissues. Enzymatic cell wall digestion and mechanical opening still provide alternative strategies to make these tissues accessible (Gilroy et al., 1986; Kuchitsu et al., 2002), but certainly represent invasive approaches that need to be tightly evaluated through the use of appropriate controls. The subcellular distribution of SMFIs can also differ between model organisms: an example are the widely-used pH indicators of the fluorescein family accumulate in the cytoplasm of mammalian cells, whereas in plants and fungi, they are efficiently sequestered to vacuoles (Slayman et al., 1994). In *Arabidopsis,* these dyes have therefore become valuable tools to measure vacuolar pH in intact roots (Krebs et al., 2010), but have also been established as vacuolar lumen stains to study vacuole biogenesis and to obtain detailed three-dimensional reconstructions of plant vacuoles (Kriegel et al., 2015; Viotti et al., 2013). A summary of challenges and solutions when using fluorescent indicators in plant cells can be found in Table 1.

Journal of Cell Science (2018) 131, jcs209270. doi:10.1242/jcs.209270

Table 2. Examples of fluorescent indicator applications in plants

Parameter measured	Fluorescent indicator	Indicator type	Example applications in plants	References
Ca^{2+}[a]	Indo-1	SMFI	$[Ca^{2+}]_{Cyt}$ in guard cells and roots of *Arabidopsis* and in barley aleurone cells	Bush and Jones, 1987; Grynkiewicz et al., 1985[b]; Legue et al., 1997
	Calcium Green-1	SMFI	$[Ca^{2+}]_{Cyt}$ in guard cells of *Arabidopsis* and *Commelina*	Eberhard and Erne, 1991; Kuchitsu et al., 2002[b]
	Fura-2	SMFI	$[Ca^{2+}]_{Cyt}$ in guard cells of *Arabidopsis* and *Commelina*	Allen et al., 1999a; Grynkiewicz et al., 1985[b]; Kuchitsu et al., 2002
	Yellow Cameleon-based indicators	GEFI	$[Ca^{2+}]_{cyt}$ in *Arabidopsis* guard cells, roots, leaves, pollen tubes; $[Ca^{2+}]_{ER}$ in *Arabidopsis* roots; $[Ca^{2+}]_{Mito}$ in *Arabidopsis* roots	Allen et al., 1999b; Bonza et al., 2013; Choi et al., 2014; Horikawa et al., 2010[b]; Iwano et al., 2009; Krebs et al., 2012; Miyawaki et al., 1997[b]; Nagai et al., 2004[b]; Palmer et al., 2006[b]; Wagner et al., 2015
	Troponin C-based indicators/Twitchs	GEFI	$[Ca^{2+}]_{Cyt}$ in *Arabidopsis* roots and female gametophyte	Denninger et al., 2014; Heim et al., 2007[b]; Thestrup et al., 2014[b]; Waadt et al., 2017
	GCaMP-based indicators	GEFI	$[Ca^{2+}]_{Cyt}$ in *Physcomitrella* and in *Arabidopsis* roots and leaves	Ast et al., 2017; Chen et al., 2013[b]; Kleist et al., 2017; Tian et al., 2009[b]; Vincent et al., 2017; Waadt et al., 2017
	GECO-based indicators	GEFI	$[Ca^{2+}]_{Cyt}$ in *Arabidopsis* roots, leaves and pollen tubes	Keinath et al., 2015; Ngo et al., 2014; Waadt et al., 2017; Zhao et al., 2011[b]
pH[a]	Fluorescein-based pH indicators (e.g. BCECF)	SMFI	$[pH]_{Vac}$ in *Arabidopsis* roots and barley aleurone cells	Krebs et al., 2010; Rink et al., 1982[b]; Swanson and Jones, 1996
	HPTS	SMFI	$[pH]_{Apo}$ in *Arabidopsis* roots	Barbez et al., 2017; [b]Zhujun and Seitz, 1984
	Ratiometric pHluorin-based indicators	GEFI	$[pH]_{Cyt}$, $[pH]_{ER}$, $[pH]_{TGN}$, $[pH]_{Golgi}$ in *Nicotiana* leaves, *Arabidopsis* roots and *Arabidopsis* protoplasts; $[pH]_{Chl}$, $[pH]_{Per}$, $[pH]_{Mito}$, $[pH]_{Nuc}$ in *Arabidopsis* protoplasts	Fendrych et al., 2014; Martinière et al., 2013b; Miesenböck et al., 1998[b]; Moseyko and Feldman, 2001; Shen et al., 2013
	pHusion-based indicators	GEFI	$[pH]_{Cyt}$ and $[pH]_{Apo}$ in *Arabidopsis* roots, leaves and hypocotyl; $[pH]_{TGN}$ in *Arabidopsis* roots	Fendrych et al., 2016; Gjetting et al., 2012[b]; Luo et al., 2015
	GFP (H148D)	GEFI	$[pH]_{Cyt}$ in *Arabidopsis* roots	Elsliger et al., 1999[b]; Fasano et al., 2001; Monshausen et al., 2009
Potassium	PBFI	SMFI	$[K^+]_{Cyt}$ in *Arabidopsis* root hairs; $[K]_{Vac}$ in *Arabidopsis* roots	Bassil et al., 2011; Halperin and Lynch, 2003; Minta and Tsien, 1989[b]
Sodium	SBFI	SMFI	$[Na^+]_{Cyt}$ in *Arabidopsis* root hairs; $[Na]_{Cyt}$ in rice protoplasts	Halperin and Lynch, 2003; Kader and Lindberg, 2005; Minta and Tsien, 1989[b]
	CoroNa Green	SMFI	$[Na^+]_{Vac}$ in roots of *Arabidopsis* and *Thellungiella* roots	Meier et al., 2006[b]; Oh et al., 2009; Park et al., 2009
Chloride	Clomeleon	GEFI	$[Cl^-]_{Cyt}$ in roots of *Arabidopsis*	Kuner and Augustine, 2000[b]; Lorenzen et al., 2004
Zinc	Zinppyr-1	SMFI	$[Zn^{2+}]_{Int}$ in *Arabidopsis* roots	Sinclair et al., 2007; Song et al., 2010; Walkup et al., 2000[b]
	eCALWY indicators	GEFI	$[Zn^{2+}]_{Cyt}$ in *Arabidopsis* roots	Lanquar et al., 2014; Vinkenborg et al., 2009[b]
ROS/redox[a]	Fluorescein-based ROS indicators (e.g. H_2DCFDA; OxyBurst Green-H_2HFF-BSA)	SMFI	$[ROS]_{Int}$ in *Arabidopsis* roots, root hairs, guard cells, pollen tubes, female gametophyte; $[ROS]_{Int}$ in maize leaves; $[ROS]_{Apo}$ in germinating radish seeds, *Arabidopsis* roots, pollen tubes and in tomato roots	Cárdenas et al., 2008; Duan et al., 2014; Han et al., 2015; Hao et al., 2012; Ivanchenko et al., 2013; Kaya et al., 2014; Monshausen et al., 2007; Monshausen et al., 2009; Rodríguez et al., 2002; Schopfer et al., 2001
	HyPer-based indicators	GEFI	$[ROS]_{Cyt}$ in *Arabidopsis* guard cells and roots; $[ROS]_{Per}$ in *Arabidopsis* guard cells	Belousov et al., 2006[b]; Costa et al., 2010; Hernández-Barrera et al., 2015; Rodrigues et al., 2017
	roGFP-based indicators	GEFI	$[E_{GSH}]_{Cyt}$ in *Arabidopsis* roots, leaves and *Nicotiana* leaves; $[E_{GSH}]_{Mito}$ in *Arabidopsis* roots and leaves; $[E_{GSH}]_{Chl}$ in *Arabidopsis* leaves; $[E_{GSH}]_{ER}$ in *Arabidopsis* and *Nicotiana* leaves; $[E_{GSH}]_{Per}$ in *Arabidopsis* and *Nicotiana* leaves	Dubreuil-Maurizi et al., 2011; Fuchs et al., 2016; Gutscher et al., 2008[b]; Hanson et al., 2004[b]; Jiang et al., 2006; Marty et al., 2009; Schwarzländer et al., 2008
ATP	ATeam1.03-nD/nA	GEFI	$[ATP]_{Cyt}$ in *Arabidopsis* whole seedlings, roots, hypocotyls, cotyledons, leaves, root hairs; $[ATP]_{Mito}$ in isolated mitochondria from whole seedlings	De Col et al., 2017; Imamura et al., 2009[b]; Kotera et al., 2010[b]
Glucose	FLIPglu indicators	GEFI	$[Gluc]_{Cyt}$ in *Arabidopsis* roots and leaves	Deuschle et al., 2006; Fehr et al., 2003[b]
Sucrose	FLIPsuc indicators	GEFI	$[Suc]_{Cyt}$ in *Arabidopsis* roots	Chaudhuri et al., 2008; Lager et al., 2006[b]
Arginine	QBP	GEFI	$[Arg]_{Cyt}$ in *Arabidopsis* roots	Bogner and Ludewig, 2007[b]
Glutamine	QBP(D157N)	GEFI	$[Gln]_{Cyt}$ in *Arabidopsis* roots	Yang et al., 2010[b]
Abscisic acid	ABACUS	GEFI	$[ABA]_{Cyt}$ and $[ABA]_{Nuc}$ in *Arabidopsis* roots and hypocotyls	Jones et al., 2014[b]
	ABAleon indicators	GEFI	$[ABA]_{Cyt}$ in *Arabidopsis* whole seedlings, roots, hypocotyls and leaves	Waadt et al., 2014[b]
Gibberellic acid	GPS1	GEFI	$[GA]_{Nuc}$ in *Arabidopsis* roots and hypocotyls	Rizza et al., 2017[b]

Cyt, cytosol; Nuc, nucleus; ER, endoplasmic reticulum; Mito, mitochondria; Vac, vacuole; Apo, apoplast; TGN, *trans*-Golgi network; Chl, Chlorplast; Per, Peroxisome; ABA, abscisic acid; GA, gibberellic acid; Gluc, Glucose; Suc, Sucrose, Int, intracellular (not compartment-specific); ROS, reactive oxygen species; E_{GSH}, glutathione redox potential.

[a]Comprehensive reviews for Ca^{2+}, pH and ROS/redox indicator applications in plants can be found elsewhere (Choi et al., 2012; Gjetting et al., 2013; Martinière et al., 2013a; Ortega-Villasante et al., 2016; Swanson et al., 2011); [b]Cites original reference for fluorescent indicator.

A better spatial control than for SMFIs is achieved by using genetically encoded fluorescent indicators (GEFIs). Their spatio-temporal expression and cellular localization can be precisely controlled by the use of appropriate promoters and targeting sequences, which enable selective analyses of different tissues, cell types and compartments (Table 2). The majority of available GEFIs have been developed and enhanced *in vitro* and functionally tested in mammalian cells (Miesenböck et al., 1998; Tantama et al., 2013; Thestrup et al., 2014). The transfer of GEFI applications to plant model organisms worked in many cases without further engineering, because critical improvements of fluorescent protein properties, such as removal of the cryptic intron, protein stability and codon optimization, had been established early on (Davis and Vierstra, 1998; Haseloff et al., 1997; Siemering et al., 1996). The use of the strong cauliflower mosaic virus *35S* promoter for high-level GEFI expression in plants has repeatedly led to complications owing to post-transcriptional gene silencing (Daxinger et al., 2008). This issue has been addressed by the use of alternative promoters (e.g. *UBQ10*), or by introducing GEFIs in a silencing-deficient genetic background (Deuschle et al., 2006; Krebs et al., 2012). The cell type-specific expression of sensors can further improve sensitivity in cases where signals of surrounding cells could interfere with measurements in deeper tissue layers. This approach was successfully applied in *Arabidopsis* for the recording of Ca^{2+} signaling events during the double fertilization of egg cell and central cell (Denninger et al., 2014; Hamamura et al., 2014), which are hidden inside the ovule and enclosed by layers of integuments.

With regard to the applications of fluorescent indicators, these are intimately linked to the development of appropriate technical accessories that guarantee stable environmental conditions over prolonged periods. As mentioned above, different types of perfusion chambers, setups for vertical-stage microscopy, custom-made software and techniques for local stimulus applications are prerequisites for the successful application of fluorescent indicators in intact seedlings (Grossmann et al., 2011; Krebs and Schumacher, 2013; Poxson et al., 2017; von Wangenheim et al., 2017).

Fluorescent indicator applications in plants have allowed researchers to gain new insights into different aspects of plant physiology and cell biology. An example that exploits the full potential of the fluorescent indicator technology is the analysis of intracellular ATP levels (De Col et al., 2017). The applications range from *ex situ* functional assays on isolated mitochondria, to *in vivo* cytoplasmic ATP mapping on a whole-seedling scale, which provides us with an integrated view on ATP-related energy metabolism in *Arabidopsis* (De Col et al., 2017).

Other fluorescent indicator applications have shed new light on long-standing questions in plant biology: the acid-growth hypothesis, proposed in the 1970s (Hager et al., 1971; Rayle and Cleland, 1970), postulated that cell expansion is enabled through apoplastic acidification that is triggered by auxin. The application of different pH-sensitive fluorescent indicators in the apoplast of *Arabidopsis* roots and hypocotyls has now significantly strengthened this hypothesis (Barbez et al., 2017; Fendrych et al., 2016). Such targeting of fluorescent indicators to cellular compartments, such as the apoplast, underlines the importance of assessing local biophysical and biochemical cellular environments. With the discovery of the organization of protein complexes in microdomains and nanodomains, this is becoming increasingly important (Bücherl et al., 2017). A future challenge will be the precise spatial analysis (mainly along the *z*-axis) of cellular micro-environments that are in close proximity to the plasma membrane, as shown for a sub-population of mitochondria during plant cell infection that exhibit an altered redox state compared to more distant organelles (Fuchs et al., 2016).

Beside the requirement for increased spatial resolution, future fluorescent indicator applications will have to cover the simultaneous measurement of multiple parameters. For example, long-distance signal propagation during salt stress involves at least two types of signaling molecules: Ca^{2+} and reactive oxygen species (ROS) (Choi et al., 2014; Evans et al., 2016). It is still not clear whether salt-induced long-distance signals are solely driven by Ca^{2+} and ROS, or whether electrical signals could be involved as well (Choi et al., 2017). To gain insights into the order of events and the interdependent behavior of different signaling molecules, multiparameter imaging is required, which has been recently established in *Arabidopsis* to simultaneously monitor Ca^{2+} and abscisic acid (Waadt et al., 2017).

Finally, it will be important to convert qualitative fluorescent indicator readouts into quantitative data that can be linked to the biochemical properties of the molecular players that are involved in a particular signaling pathway or a physiological process. The calibration of fluorescent indicators in a multi-cellular plant context is certainly not trivial, but has been successfully reported for indicators to monitor pH, Ca^{2+} and redox state (Jiang et al., 2006; Krebs et al., 2010; Legue et al., 1997; Martinière et al., 2013b; Moseyko and Feldman, 2001; Schwarzländer et al., 2008; Waadt et al., 2017) (Table 2).

In summary, fluorescent indicator applications have become essential and established tools to study physiological and cellular processes in living plant cells. Future efforts in this field will have to focus on the advancement of imaging techniques to be able to study cellular environments at the nanoscale level. Furthermore, implementation of calibration techniques and multiplex imaging will be required to advance our understanding of complex signaling and metabolic networks in plant cells.

Protein interactions and complex compositions measured by fluorescence lifetime and anisotropy

Förster resonance energy transfer (FRET) measurements provide a very precise and powerful way to measure protein–protein interactions *in vivo* with highest resolution in 3D (Förster, 1948; Lakowicz, 2006). For FRET, the two proteins of interest have to be expressed in fusion with appropriate, spectrally distinct fluorescent proteins, so-called FRET pairs (e.g. CFP/YFP, GFP/RFP or GFP/mCherry). For the necessary energy transfer from the excited donor fluorescent protein to the acceptor protein, the donor has to have a substantial overlap of its emission spectrum with the excitation spectrum of the acceptor. FRET depends on the close distance of the two fluorescent proteins to each other, which is usually in the range of 5–10 nm; this is well below the diffraction limit of a confocal microscope, and can therefore be used as an indicator for physical protein–protein interactions (Förster, 1948; Lakowicz, 2006).

One robust, minimally-invasive way to quantitatively measure FRET (apart from intensity-based measurements, such as acceptor photobleaching or ratiometric imaging) is to determine the fluorescence lifetime of the donor by employing fluorescence lifetime imaging microscopy (FLIM). The mean fluorescence lifetime τ of the molecule is defined by its average time that it remains in the excited state before it returns to its ground state, thereby emitting a photon; this usually lies in the nanosecond range. In the case of FRET, the mean τ of the donor is reduced, because energy is transferred to the acceptor, which then emits fluorescent photons. The recent overview by Weidtkamp-Peters and Stahl

Journal of Cell Science (2018) 131, jcs209270. doi:10.1242/jcs.209270

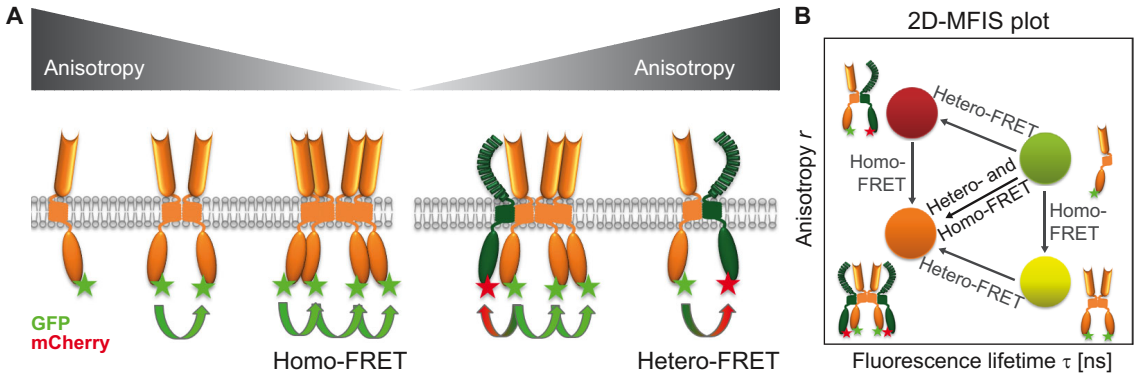

Fig. 3. Protein complex formation measurements through anisotropy and MFIS. (A) Fluorescence anisotropy measurements help to uncover homomeric and heteromeric protein complex formation. In case of protein homo-oligomerization, homo-FRET can take place and the fluorescence anisotropy is decreasing. In case of protein hetero-oligomerization, hetero-FRET occurs, and the anisotropy is increasing. (B) Data acquired by MFIS for the simultaneous acquisition of fluorescence lifetime and anisotropy can be plotted in a 2D graph for better visualization. Homomerization and heteromerization of protein complexes can be easily visualized as distinct populations.

provides more theoretical and practical details on FRET and FRET-FLIM measurements in plants (Weidtkamp-Peters and Stahl, 2017).

Protein–protein interaction measurements through FRET-FLIM with endogenous levels of fluorescently labeled proteins are desirable and can be achieved by expressing fluorescently labeled, functional proteins by their endogenous promoters in null mutant backgrounds (e.g. in stably transformed *Arabidopsis thaliana*). This provides the grounds for gaining important insights into complex formations inside the relevant tissues, and even in subcellular compartments in native conditions. These studies can reveal tissue- and cell-type specific differences for protein–protein interactions and unravel the partitioning of specific protein-protein interactions and complex compositions that are necessary for the consequent biological output, such as cell specification, growth and development (Bücherl et al., 2013; Laursen et al., 2016; Long et al., 2017). Even transient expression systems, such as the leaf epidermal cells of *Nicotiana benthamiana,* can provide fast means of FRET measurements in plants at near-endogenous expression levels by using inducible promoters (Bleckmann et al., 2010; Somssich et al., 2015; Stahl et al., 2013).

Moreover, the use of multiparameter fluorescence imaging spectroscopy (MFIS) allows the differentiation between homomeric and heteromeric protein complexes (Weidtkamp-Peters et al., 2009) (Fig. 3). Here, the fluorescent lifetime τ and fluorescent anisotropy *r* are measured at the same time in every pixel of the acquired image. Thus, even dynamic measurements of the same cells are possible over time as FRET-FLIM and anisotropy measurements only require non-invasive, low-excitation powers of a pulsed laser source due to the highly sensitive single-photon counting detectors that are used (Somssich et al., 2015; Stahl et al., 2013; Weidtkamp-Peters et al., 2009).

Fluorescence anisotropy *r* is a fundamental property (as is the fluorescence lifetime τ) of a given fluorescent protein and describes its depolarization. The fluorescence anisotropy changes depending on the rotational freedom of the molecule. In the case of hetero-FRET (FRET between donor and acceptor, which indicates heteromeric complex formation) (Fig. 3A), the labelled proteins usually have less rotational freedom than non-interacting proteins, so the anisotropy increases (polarization). In the case of homo-FRET (FRET between donors only, which indicates homomeric complex formation), the anisotropy decreases, because of the transfer of energy to slightly differently oriented donor molecules in close proximity (depolarization) (Fig. 3B) (Bader et al., 2011; Borst and Visser, 2010). Of course, both heteromeric and homomeric complexes can occur at the same time, which leads to reduced fluorescent lifetimes and reduced fluorescent anisotropy values. This can be deduced pixel-wise and utilized to unravel differential protein complexes, and visualized with the use of 2D plots (Fig. 3B) (Somssich et al., 2015; Stahl et al., 2013). Other fluorescence correlation spectroscopy (FCS)-based techniques, such as fluorescence cross correlation spectroscopy (FCCS) or scanning FCS in combination with brightness analyses, have recently been used to investigate the mobility, oligomeric state and stoichiometry of protein complexes in plants (Clark et al., 2016; Laursen et al., 2016; Wang et al., 2015a) (see Glossary).

In summary, FRET-FLIM, anisotropy and FCS measurements have been successfully used to uncover protein–protein interactions and complex compositions in a dynamic and minimally invasive way, both in transient plant expression systems and in stable transgenic lines.

Conclusions

Constant efforts of multiple research groups in adapting novel imaging techniques or developing custom devices that allow non-invasive plant growth on microscope-compatible supports have greatly accelerated plant cell imaging over the last decade (Shaw and Ehrhardt, 2013). These methods now allow to explore challenging biological questions in living cells and multicellular tissues, such as spatio-temporal dynamics and organization of cellular subcompartments, the stoichiometry of multi-component protein complexes, cell and tissue plasticity on the level of proteins, metabolites and physiological parameters, image-based flux analyses and others. Whereas these tasks are not only methodologically demanding, such approaches will also help to further develop and refine existing and upcoming technologies with the long-term goal to make them available to a broad scientific community. However, with the rapid advancements in modern fluorescence microscopy, user-friendly imaging setups, and the resulting increased SNR, standard confocal systems are commonly purchased and frequently used without the necessary caution during image acquisition. This can result in a tremendous increase in published cell biological data with sometimes alarming over interpretation or misinterpretation of the presented data. Therefore, statistically sound image quantifications, together with a detailed description of any digital image processing (Jarsch and

Ott, 2015) need to become an inevitable standard in plant cell biology. In addition, detailed technical descriptions and drawings for engineering, as deposited in freely accessible repositories, or as recently published (von Wangenheim et al., 2017), are essential steps to drive innovations in this rapidly evolving field.

Competing interests

The authors declare no competing or financial interests.

Funding

The work of our laboratories has been supported by individual grants of the German Research Foundation (Deutsche Forschungsgemeinschaft, DFG) to A.M. (MA5293/2-1 and MA5293/6-1), T.O. (INST 95/1126-2, B04; Sonderforschungsbereich 924), Y.S. (STA12/12 1-1), M.K. (KR4675/2-1) and G.G. (GR4559/3-1), the Excellence Cluster CellNetworks (G.G.), and the Boehringer Ingelheim Foundation (A.M.). J.E.M.V. is supported by Swiss National Science Foundation (Schweizerischer Nationalfonds zur Förderung der Wissenschaftlichen Forschung) (PP00P3_157524 and 316030_164086) and the Netherlands Organization for Scientific Research (Nederlandse Organisatie voor Wetenschappelijk Onderzoek) (NWO 864.13.008).

References

Allen, G. J., Kuchitsu, K., Chu, S. P., Murata, Y. and Schroeder, J. I. (1999a). Arabidopsis abi1-1 and abi2-1 phosphatase mutations reduce abscisic acid-induced cytoplasmic calcium rises in guard cells. *Plant Cell* **11**, 1785-1798.

Allen, G. J., Kwak, J. M., Chu, S. P., Llopis, J., Tsien, R. Y., Harper, J. F. and Schroeder, J. I. (1999b). Cameleon calcium indicator reports cytoplasmic calcium dynamics in Arabidopsis guard cells. *Plant J.* **19**, 735-747.

Ast, C., Foret, J., Oltrogge, L. M., De Michele, R., Kleist, T. J., Ho, C.-H. and Frommer, W. B. (2017). Ratiometric Matryoshka biosensors from a nested cassette of green- and orange-emitting fluorescent proteins. *Nat. Commun.* **8**, 431.

Bader, A. N., Hoetzl, S., Hofman, E. G., Voortman, J., van Bergen en Henegouwen, P. M. P., van Meer, G. and Gerritsen, H. C. (2011). Homo-FRET imaging as a tool to quantify protein and lipid clustering. *Chemphyschem* **12**, 475-483.

Barbez, E., Dünser, K., Gaidora, A., Lendl, T. and Busch, W. (2017). Auxin steers root cell expansion via apoplastic pH regulation in Arabidopsis thaliana. *Proc. Natl. Acad. Sci. USA* **114**, E4884-E4893.

Barbier de Reuille, P., Routier-Kierzkowska, A.-L., Kierzkowski, D., Bassel, G. W., Schüpbach, T., Tauriello, G., Bajpai, N., Strauss, S., Weber, A., Kiss, A. et al. (2015). MorphoGraphX: A platform for quantifying morphogenesis in 4D. *Elife* **4**, e05864.

Bascom, C. S., Jr, Wu, S.-Z., Nelson, K., Oakey, J. and Bezanilla, M. (2016). Long-term growth of moss in microfluidic devices enables subcellular studies in development. *Plant Physiol.* **172**, 28-37.

Bassil, E., Tajima, H., Liang, Y.-C., Ohto, M.-A., Ushijima, K., Nakano, R., Esumi, T., Coku, A., Belmonte, M. and Blumwald, E. (2011). The Arabidopsis Na+/H+ antiporters NHX1 and NHX2 control vacuolar pH and K+ homeostasis to regulate growth, flower development, and reproduction. *Plant Cell* **23**, 3482-3497.

Belousov, V. V., Fradkov, A. F., Lukyanov, K. A., Staroverov, D. B., Shakhbazov, K. S., Terskikh, A. V. and Lukyanov, S. (2006). Genetically encoded fluorescent indicator for intracellular hydrogen peroxide. *Nat. Methods* **3**, 281-286.

Berson, T., von Wangenheim, D., Takáč, T., Šamajová, O., Rosero, A., Ovečka, M., Komis, G., Stelzer, E. H. K. and Šamaj, J. (2014). Trans-Golgi network localized small GTPase RabA1d is involved in cell plate formation and oscillatory root hair growth. *BMC Plant Biol.* **14**, 252.

Berthet, B. and Maizel, A. (2016). Light sheet microscopy and live imaging of plants. *J. Microscopy* **263**, 158-164.

Birnbaum, K., Shasha, D. E., Wang, J. Y., Jung, J. W., Lambert, G. M., Galbraith, D. W. and Benfey, P. N. (2003). A gene expression map of the Arabidopsis root. *Science* **302**, 1956-1960.

Bleckmann, A., Weidtkamp-Peters, S., Seidel, C. A. M. and Simon, R. (2010). Stem cell signaling in Arabidopsis requires CRN to localize CLV2 to the plasma membrane. *Plant Physiol.* **152**, 166-176.

Bogner, M. and Ludewig, U. (2007). Visualization of arginine influx into plant cells using a specific FRET-sensor. *J. Fluoresc.* **17**, 350-360.

Bonza, M. C., Loro, G., Behera, S., Wong, A., Kudla, J. and Costa, A. (2013). Analyses of Ca2+ accumulation and dynamics in the endoplasmic reticulum of Arabidopsis root cells using a genetically encoded Cameleon sensor. *Plant Physiol.* **163**, 1230-1241.

Borlinghaus, R. T. and Kappel, C. (2016). HyVolution—the smart path to confocal superresolution. *Nat. Methods* **13**, nmeth.f.392.

Borst, J. W. and Visser, A. J. W. G. (2010). Fluorescence lifetime imaging microscopy in life sciences. *Measurement Sci. Technol.* **21**, 102002.

Brakenhoff, G. J., Muller, M. and Ghauharali, R. I. (1996). Analysis of efficiency of two-photon versus single-photon absorption for fluorescence generation in biological objects. *J. Microscopy.* **183**, 140-144.

Bücherl, C. A., van Esse, G. W., Kruis, A., Luchtenberg, J., Westphal, A. H., Aker, J., van Hoek, A., Albrecht, C., Borst, J. W. and de Vries, S. C. (2013). Visualization of BRI1 and BAK1(SERK3) membrane receptor heterooligomers during brassinosteroid signaling. *Plant Physiol.* **162**, 1911-1925.

Bücherl, C. A., Jarsch, I. K., Schudoma, C., Segonzac, C., Mbengue, M., Robatzek, S., MacLean, D., Ott, T. and Zipfel, C. (2017). Plant immune and growth receptors share common signalling components but localise to distinct plasma membrane nanodomains. *Elife* **6**, e25114.

Busch, W., Moore, B. T., Martsberger, B., Mace, D. L., Twigg, R. W., Jung, J., Pruteanu-Malinici, I., Kennedy, S. J., Fricke, G. K., Clark, R. L. et al. (2012). A microfluidic device and computational platform for high-throughput live imaging of gene expression. *Nat. Methods* **9**, 1101-1106.

Bush, D. S. and Jones, R. L. (1987). Measurement of cytoplasmic calcium in aleurone protoplasts using Indo-1 and Fura-2. *Cell Calcium* **8**, 455-472.

Cárdenas, L., Martínez, A., Sánchez, F. and Quinto, C. (2008). Fast, transient and specific intracellular ROS changes in living root hair cells responding to Nod factors (NFs). *Plant J.* **56**, 802-813.

Chaudhuri, B., Hörmann, F., Lalonde, S., Brady, S. M., Orlando, D. A., Benfey, P. and Frommer, W. B. (2008). Protonophore- and pH-insensitive glucose and sucrose accumulation detected by FRET nanosensors in Arabidopsis root tips. *Plant J.* **56**, 948-962.

Chen, T.-W., Wardill, T. J., Sun, Y., Pulver, S. R., Renninger, S. L., Baohan, A., Schreiter, E. R., Kerr, R. A., Orger, M. B., Jayaraman, V. et al. (2013). Ultrasensitive fluorescent proteins for imaging neuronal activity. *Nature* **499**, 295-300.

Choi, W.-G., Toyota, M., Kim, S.-H., Hilleary, R. and Gilroy, S. (2014). Salt stress-induced Ca2+ waves are associated with rapid, long-distance root-to-shoot signaling in plants. *Proc. Natl. Acad. Sci. USA* **111**, 6497-6502.

Choi, W.-G., Miller, G., Wallace, I., Harper, J., Mittler, R. and Gilroy, S. (2017). Orchestrating rapid long-distance signaling in plants with Ca2+, ROS and electrical signals. *Plant J.* **90**, 698-707.

Choi, W. G., Swanson, S. J. and Gilroy, S. (2012). High-resolution imaging of Ca2+, redox status, ROS and pH using GFP biosensors. *Plant J.* **70**, 118-128.

Clark, N. M., Hinde, E., Winter, C. M., Fisher, A. P., Crosti, G., Blilou, I., Gratton, E., Benfey, P. N. and Sozzani, R. (2016). Tracking transcription factor mobility and interaction in Arabidopsis roots with fluorescence correlation spectroscopy. *Elife* **5**, e14770.

Costa, A., Drago, I., Behera, S., Zottini, M., Pizzo, P., Schroeder, J. I., Pozzan, T. and Lo Schiavo, F. (2010). H2O2 in plant peroxisomes: an in vivo analysis uncovers a Ca(2+)-dependent scavenging system. *Plant J.* **62**, 760-772.

Costa, A., Candeo, A., Fieramonti, L., Valentini, G. and Bassi, A. (2013). Calcium dynamics in root cells of Arabidopsis thaliana visualized with selective plane illumination microscopy. *PLoS ONE* **8**, e75646.

Davis, S. J. and Vierstra, R. D. (1998). Soluble, highly fluorescent variants of green fluorescent protein (GFP) for use in higher plants. *Plant Mol. Biol.* **36**, 521-528.

Daxinger, L., Hunter, B., Sheikh, M., Jauvion, V., Gasciolli, V., Vaucheret, H., Matzke, M. and Furner, I. (2008). Unexpected silencing effects from T-DNA tags in Arabidopsis. *Trends Plant Sci.* **13**, 4-6.

De Col, V., Fuchs, P., Nietzel, T., Elsässer, M., Voon, C. P., Candeo, A., Seeliger, I., Fricker, M. D., Grefen, C., Møller, I. M. et al. (2017). ATP sensing in living plant cells reveals tissue gradients and stress dynamics of energy physiology. *Elife* **6**, e26770.

de Luis Balaguer, M. A., Ramos-Pezzotti, M., Rahhal, M. B., Melvin, C. E., Johannes, E., Horn, T. J. and Sozzani, R. (2016). Multi-sample Arabidopsis Growth and Imaging Chamber (MAGIC) for long term imaging in the ZEISS Lightsheet Z.1. *Dev. Biol.* **419**, 19-25.

de Medeiros, G., Norlin, N., Gunther, S., Albert, M., Panavaite, L., Fiuza, U.-M., Peri, F., Hiiragi, T., Krzic, U. and Hufnagel, L. (2015). Confocal multiview light-sheet microscopy. *Nat. Commun.* **6**, 8881.

De Rybel, B., Vassileva, V., Parizot, B., Demeulenaere, M., Grunewald, W., Audenaert, D., Van Campenhout, J., Overvoorde, P., Jansen, L., Vanneste, S. et al. (2010). A novel aux/IAA28 signaling cascade activates GATA23-dependent specification of lateral root founder cell identity. *Curr. Biol.* **20**, 1697-1706.

De Storme, N. and Geelen, D. (2014). The impact of environmental stress on male reproductive development in plants: biological processes and molecular mechanisms. *Plant Cell Environ.* **37**, 1-18.

Denk, W., Strickler, J. H. and Webb, W. W. (1990). Two-photon laser scanning fluorescence microscopy. *Science* **248**, 73-76.

Denninger, P., Bleckmann, A., Lausser, A., Vogler, F., Ott, T., Ehrhardt, D. W., Frommer, W. B., Sprunck, S., Dresselhaus, T. and Grossmann, G. (2014). Male-female communication triggers calcium signatures during fertilization in Arabidopsis. *Nat. Commun.* **5**, 4645.

Deuschle, K., Chaudhuri, B., Okumoto, S., Lager, I., Lalonde, S. and Frommer, W. B. (2006). Rapid metabolism of glucose detected with FRET glucose nanosensors in epidermal cells and intact roots of Arabidopsis RNA-silencing mutants. *Plant Cell* **18**, 2314-2325.

Drobizhev, M., Tillo, S., Makarov, N. S., Hughes, T. E. and Rebane, A. (2009). Absolute two-photon absorption spectra and two-photon brightness of orange and red fluorescent proteins. *J. Phys. Chem. B* **113**, 855-859.

Drobizhev, M., Makarov, N. S., Tillo, S. E., Hughes, T. E. and Rebane, A. (2011). Two-photon absorption properties of fluorescent proteins. *Nat. Methods* **8**, 393-399.

Duan, Q., Kita, D., Johnson, E. A., Aggarwal, M., Gates, L., Wu, H.-M. and Cheung, A. Y. (2014). Reactive oxygen species mediate pollen tube rupture to release sperm for fertilization in Arabidopsis. *Nat. Commun.* **5**, 3129.

Dubreuil-Maurizi, C., Vitecek, J., Marty, L., Branciard, L., Frettinger, P., Wendehenne, D., Meyer, A. J., Mauch, F. and Poinssot, B. (2011). Glutathione deficiency of the Arabidopsis mutant pad2-1 affects oxidative stress-related events, defense gene expression, and the hypersensitive response. *Plant Physiol.* **157**, 2000-2012.

Eberhard, M. and Erne, P. (1991). Calcium binding to fluorescent calcium indicators: calcium green, calcium orange and calcium crimson. *Biochem. Biophys. Res. Commun.* **180**, 209-215.

Elsliger, M.-A., Wachter, R. M., Hanson, G. T., Kallio, K. and Remington, S. J. (1999). Structural and spectral response of green fluorescent protein variants to changes in pH. *Biochemistry* **38**, 5296-5301.

Evans, M. J., Choi, W.-G., Gilroy, S. and Morris, R. J. (2016). A ROS-assisted calcium wave dependent on the AtRBOHD NADPH oxidase and TPC1 cation channel propagates the systemic response to salt stress. *Plant Physiol.* **171**, 1771-1784.

Fasano, J. M., Swanson, S. J., Blancaflor, E. B., Dowd, P. E., Kao, T. H. and Gilroy, S. (2001). Changes in root cap pH are required for the gravity response of the Arabidopsis root. *Plant Cell* **13**, 907-921.

Fehr, M., Lalonde, S., Lager, I., Wolff, M. W. and Frommer, W. B. (2003). In vivo imaging of the dynamics of glucose uptake in the cytosol of COS-7 cells by fluorescent nanosensors. *J. Biol. Chem.* **278**, 19127-19133.

Feijo, J. A. and Moreno, N. (2004). Imaging plant cells by two-photon excitation. *Protoplasma* **223**, 1-32.

Fendrych, M., Van Hautegem, T., Van Durme, M., Olvera-Carrillo, Y., Huysmans, M., Karimi, M., Lippens, S., Guérin, C. J., Krebs, M., Schumacher, K. et al. (2014). Programmed cell death controlled by ANAC033/SOMBRERO determines root cap organ size in Arabidopsis. *Curr. Biol.* **24**, 931-940.

Fendrych, M., Leung, J. and Friml, J. (2016). TIR1/AFB-Aux/IAA auxin perception mediates rapid cell wall acidification and growth of Arabidopsis hypocotyls. *Elife* **5**, e19048.

Fernandez, R., Das, P., Mirabet, V., Moscardi, E., Traas, J., Verdeil, J.-L., Malandain, G. and Godin, C. (2010). Imaging plant growth in 4D: robust tissue reconstruction and lineaging at cell resolution. *Nat. Methods* **7**, 547-553.

Fischer, U., Ikeda, Y., Ljung, K., Serralbo, O., Singh, M., Heidstra, R., Palme, K., Scheres, B. and Grebe, M. (2006). Vectorial information for Arabidopsis planar polarity is mediated by combined AUX1, EIN2, and GNOM activity. *Curr. Biol.* **16**, 2143-2149.

Förster, T. (1948). Zwischenmolekulare Energiewanderung und Fluoreszenz. *Ann. Phys.* **437**, 55-75.

Fournier, J., Timmers, A. C. J., Sieberer, B. J., Jauneau, A., Chabaud, M. and Barker, D. G. (2008). Mechanism of infection thread elongation in root hairs of Medicago truncatula and dynamic interplay with associated rhizobial colonization. *Plant Physiol.* **148**, 1985-1995.

Froelich, D. R., Mullendore, D. L., Jensen, K. H., Ross-Elliott, T. J., Anstead, J. A., Thompson, G. A., Pelissier, H. C. and Knoblauch, M. (2011). Phloem ultrastructure and pressure flow: Sieve-Element-Occlusion-Related agglomerations do not affect translocation. *Plant Cell* **23**, 4428-4445.

Fuchs, R., Kopischke, M., Klapprodt, C., Hause, G., Meyer, A. J., Schwarzlander, M., Fricker, M. D. and Lipka, V. (2016). Immobilized subpopulations of leaf epidermal mitochondria mediate PENETRATION2-dependent pathogen entry control in arabidopsis. *Plant Cell* **28**, 130-145.

Germond, A., Fujita, H., Ichimura, T. and Watanabe, T. M. (2016). Design and development of genetically encoded fluorescent sensors to monitor intracellular chemical and physical parameters. *Biophys. Rev.* **8**, 121-138.

Gilroy, S., Hughes, W. A. and Trewavas, A. J. (1986). The measurement of intracellular calcium levels in protoplasts from higher plant cells. *FEBS Lett.* **199**, 217-221.

Gjetting, S. K., Ytting, C. K., Schulz, A. and Fuglsang, A. T. (2012). Live imaging of intra- and extracellular pH in plants using pHusion, a novel genetically encoded biosensor. *J. Exp. Bot.* **63**, 3207-3218.

Gjetting, S. K., Schulz, A. and Fuglsang, A. T. (2013). Perspectives for using genetically encoded fluorescent biosensors in plants. *Front. Plant Sci.* **4**, 234.

Goh, T., Toyokura, K., Wells, D. M., Swarup, K., Yamamoto, M., Mimura, T., Weijers, D., Fukaki, H., Laplaze, L., Bennett, M. J. et al. (2016). Quiescent center initiation in the Arabidopsis lateral root primordia is dependent on the SCARECROW transcription factor. *Development* **143**, 3363-3371.

Gooh, K., Ueda, M., Aruga, K., Park, J., Arata, H., Higashiyama, T. and Kurihara, D. (2015). Live-cell imaging and optical manipulation of Arabidopsis early embryogenesis. *Dev. Cell* **34**, 242-251.

Gronnier, J., Crowet, J.-M., Habenstein, B., Nasir, M. N., Bayle, V., Hosy, E., Platre, M. P., Gouguet, P., Raffaele, S., Martinez, D. et al. (2017). Structural basis for plant plasma membrane protein dynamics and organization into functional nanodomains. *Elife* **6**, e26404.

Grossmann, G., Guo, W.-J., Ehrhardt, D. W., Frommer, W. B., Sit, R. V., Quake, S. R. and Meier, M. (2011). The RootChip: an integrated microfluidic chip for plant science. *Plant Cell* **23**, 4234-4240.

Grossmann, G., Meier, M., Cartwright, H. N., Sosso, D., Quake, S. R., Ehrhardt, D. W. and Frommer, W. B. (2012). Time-lapse fluorescence imaging of Arabidopsis root growth with rapid manipulation of the root environment using the RootChip. *J. Vis. Exp.* **65**, 4290.

Grynkiewicz, G., Poenie, M. and Tsien, R. Y. (1985). A new generation of Ca2+ indicators with greatly improved fluorescence properties. *J. Biol. Chem.* **260**, 3440-3450.

Gutscher, M., Pauleau, A.-L., Marty, L., Brach, T., Wabnitz, G. H., Samstag, Y., Meyer, A. J. and Dick, T. P. (2008). Real-time imaging of the intracellular glutathione redox potential. *Nat. Methods* **5**, 553-559.

Hager, A., Menzel, H. and Krauss, A. (1971). Versuche und Hypothese zur Primärwirkung des Auxins beim Streckungswachstum. *Planta* **100**, 45-75.

Halperin, S. J. and Lynch, J. P. (2003). Effects of salinity on cytosolic Na+ and K+ in root hairs of Arabidopsis thaliana: in vivo measurements using the fluorescent dyes SBFI and PBFI. *J. Exp. Bot.* **54**, 2035-2043.

Hamamura, Y., Nishimaki, M., Takeuchi, H., Geitmann, A., Kurihara, D. and Higashiyama, T. (2014). Live imaging of calcium spikes during double fertilization in Arabidopsis. *Nat. Commun.* **5**, 4722.

Han, S., Fang, L., Ren, X., Wang, W. and Jiang, J. (2015). MPK6 controls H2 O2-induced root elongation by mediating Ca2+ influx across the plasma membrane of root cells in Arabidopsis seedlings. *New Phytol.* **205**, 695-706.

Hanson, G. T., Aggeler, R., Oglesbee, D., Cannon, M., Capaldi, R. A., Tsien, R. Y. and Remington, S. J. (2004). Investigating mitochondrial redox potential with redox-sensitive green fluorescent protein indicators. *J. Biol. Chem.* **279**, 13044-13053.

Hao, L.-H., Wang, W.-X., Chen, C., Wang, Y.-F., Liu, T., Li, X. and Shang, Z.-L. (2012). Extracellular ATP promotes stomatal opening of Arabidopsis thaliana through heterotrimeric G protein alpha subunit and reactive oxygen species. *Mol. Plant* **5**, 852-864.

Hao, H., Fan, L., Chen, T., Li, R., Li, X., He, Q., Botella, M. A. and Lin, J. (2014). Clathrin and membrane microdomains cooperatively regulate RbohD dynamics and activity in arabidopsis. *Plant Cell* **26**, 1729-1745.

Haseloff, J., Siemering, K. R., Prasher, D. C. and Hodge, S. (1997). Removal of a cryptic intron and subcellular localization of green fluorescent protein are required to mark transgenic Arabidopsis plants brightly. *Proc. Natl. Acad. Sci. USA* **94**, 2122-2127.

Heim, N., Garaschuk, O., Friedrich, M. W., Mank, M., Milos, R. I., Kovalchuk, Y., Konnerth, A. and Griesbeck, O. (2007). Improved calcium imaging in transgenic mice expressing a troponin C-based biosensor. *Nat. Methods* **4**, 127-129.

Hernández-Barrera, A., Velarde-Buendía, A., Zepeda, I., Sanchez, F., Quinto, C., Sánchez-Lopez, R., Cheung, A. Y., Wu, H.-M. and Cardenas, L. (2015). Hyper, a hydrogen peroxide sensor, indicates the sensitivity of the Arabidopsis root elongation zone to aluminum treatment. *Sensors (Basel)* **15**, 855-867.

Höckendorf, B., Thumberger, T. and Wittbrodt, J. (2012). Quantitative analysis of embryogenesis: a perspective for light sheet microscopy. *Dev. Cell* **23**, 1111-1120.

Horade, M., Kanaoka, M. M., Kuzuya, M., Higashiyama, T. and Kaji, N. (2013). A microfluidic device for quantitative analysis of chemoattraction in plants. *RSC Adv.* **3**, 22301.

Horikawa, K., Yamada, Y., Matsuda, T., Kobayashi, K., Hashimoto, M., Matsu-ura, T., Miyawaki, A., Michikawa, T., Mikoshiba, K. and Nagai, T. (2010). Spontaneous network activity visualized by ultrasensitive Ca(2+) indicators, yellow Cameleon-Nano. *Nat. Methods* **7**, 729-732.

Huff, J. (2015). The Airyscan detector from ZEISS: confocal imaging with improved signal-to-noise ratio and super-resolution. *Nat. Methods* **12**, nmeth.f.388.

Hutten, S. J., Hamers, D. S., Aan den Toorn, M., van Esse, W., Nolles, A., Bücherl, C. A., de Vries, S. C., Hohlbein, J. and Borst, J. W. (2017). Visualization of BRI1 and SERK3/BAK1 nanoclusters in arabidopsis roots. *PLoS ONE* **12**, e0169905.

Imamura, H., Huynh Nhat, K. P., Togawa, H., Saito, K., Iino, R., Kato-Yamada, Y., Nagai, T. and Noji, H. (2009). Visualization of ATP levels inside single living cells with fluorescence resonance energy transfer-based genetically encoded indicators. *Proc. Natl. Acad. Sci. USA* **106**, 15651-15656.

Ivanchenko, M. G., den Os, D., Monshausen, G. B., Dubrovsky, J. G., Bednářová, A. and Krishnan, N. (2013). Auxin increases the hydrogen peroxide (H2O2) concentration in tomato (Solanum lycopersicum) root tips while inhibiting root growth. *Ann. Bot.* **112**, 1107-1116.

Iwano, M., Entani, T., Shiba, H., Kakita, M., Nagai, T., Mizuno, H., Miyawaki, A., Shoji, T., Kubo, K., Isogai, A. et al. (2009). Fine-tuning of the cytoplasmic Ca2+ concentration is essential for pollen tube growth. *Plant Physiol.* **150**, 1322-1334.

Jamme, F., Kascakova, S., Villette, S., Allouche, F., Pallu, S., Rouam, V. and Réfrégiers, M. (2013). Deep UV autofluorescence microscopy for cell biology and tissue histology. *Biol. Cell* **105**, 277-288.

Jaqaman, K., Loerke, D., Mettlen, M., Kuwata, H., Grinstein, S., Schmid, S. L. and Danuser, G. (2008). Robust single-particle tracking in live-cell time-lapse sequences. *Nat. Methods* **5**, 695-702.

Jarsch, I. K. and Ott, T. (2015). Quantitative image analysis of membrane microdomains labelled by fluorescently tagged proteins in Arabidopsis thaliana and Nicotiana benthamiana. *bio-protocol* **5**, e1497.
Jarsch, I. K., Konrad, S. S. A., Stratil, T. F., Urbanus, S. L., Szymanski, W., Braun, P., Braun, K.-H. and Ott, T. (2014). Plasma membranes are subcompartmentalized into a plethora of coexisting and diverse microdomains in Arabidopsis and Nicotiana benthamiana. *Plant Cell* **26**, 1698-1711.
Jiang, K., Schwarzer, C., Lally, E., Zhang, S., Ruzin, S., Machen, T., Remington, S. J. and Feldman, L. (2006). Expression and characterization of a redox-sensing green fluorescent protein (reduction-oxidation-sensitive green fluorescent protein) in Arabidopsis. *Plant Physiol.* **141**, 397-403.
Jiang, H., Xu, Z., Aluru, M. R. and Dong, L. (2014). Plant chip for high-throughput phenotyping of Arabidopsis. *Lab. Chip* **14**, 1281-1293.
Jones, A. M., Danielson, J. A., Manojkumar, S. N., Lanquar, V., Grossmann, G. and Frommer, W. B. (2014). Abscisic acid dynamics in roots detected with genetically encoded FRET sensors. *Elife* **3**, e01741.
Kader, M. A. and Lindberg, S. (2005). Uptake of sodium in protoplasts of salt-sensitive and salt-tolerant cultivars of rice, Oryza sativa L. determined by the fluorescent dye SBFI. *J. Exp. Bot.* **56**, 3149-3158.
Kaya, H., Nakajima, R., Iwano, M., Kanaoka, M. M., Kimura, S., Takeda, S., Kawarazaki, T., Senzaki, E., Hamamura, Y., Higashiyama, T. et al. (2014). Ca2 +-activated reactive oxygen species production by Arabidopsis RbohH and RbohJ is essential for proper pollen tube tip growth. *Plant Cell* **26**, 1069-1080.
Keinath, N. F., Waadt, R., Brugman, R., Schroeder, J. I., Grossmann, G., Schumacher, K. and Krebs, M. (2015). Live Cell Imaging with R-GECO1 Sheds Light on flg22- and Chitin-Induced Transient [Ca(2+)]cyt Patterns in Arabidopsis. *Mol Plant* **8**, 1188-1200.
Kimata, Y., Higaki, T., Kawashima, T., Kurihara, D., Sato, Y., Yamada, T., Hasezawa, S., Berger, F., Higashiyama, T. and Ueda, M. (2016). Cytoskeleton dynamics control the first asymmetric cell division in Arabidopsis zygote. *Proc. Natl. Acad. Sci. USA* **113**, 14157-14162.
Kirchhelle, C. and Moore, I. (2017). A simple chamber for long-term confocal imaging of root and hypocotyl development. *J. Vis. Exp.* **123**, e55331.
Kleist, T. J., Cartwright, H. N., Perera, A. M., Christianson, M. L., Lemaux, P. G. and Luan, S. (2017). Genetically encoded calcium indicators for fluorescence imaging in the moss Physcomitrella: GCaMP3 provides a bright new look. *Plant Biotechnol. J.* **15**, 1235-1237.
Koch, K., Bhushan, B. and Barthlott, W. (2008). Diversity of structure, morphology and wetting of plant surfaces. *Soft Mat.* **4**, 1943-1963.
Kodama, Y. (2016). Time gating of chloroplast autofluorescence allows clearer fluorescence imaging in planta. *PLoS ONE* **11**, e0152484.
Komis, G., Šamajová, O., Ovečka, M. and Šamaj, J. (2015). Super-resolution microscopy in plant cell imaging. *Trends Plant Sci.* **20**, 834-843.
Konopka, C. A. and Bednarek, S. Y. (2008). Variable-angle epifluorescence microscopy: a new way to look at protein dynamics in the plant cell cortex. *Plant J.* **53**, 186-196.
Kotera, I., Iwasaki, T., Imamura, H., Noji, H. and Nagai, T. (2010). Reversible dimerization of Aequorea victoria fluorescent proteins increases the dynamic range of FRET-based indicators. *ACS Chem. Biol.* **5**, 215-222.
Krebs, M. and Schumacher, K. (2013). Live cell imaging of cytoplasmic and nuclear Ca2+ dynamics in Arabidopsis roots. *Cold Spring Harb. Protoc.* **2013**, 776-780.
Krebs, M., Beyhl, D., Gorlich, E., Al-Rasheid, K. A. S., Marten, I., Stierhof, Y.-D., Hedrich, R. and Schumacher, K. (2010). Arabidopsis V-ATPase activity at the tonoplast is required for efficient nutrient storage but not for sodium accumulation. *Proc. Natl. Acad. Sci. USA* **107**, 3251-3256.
Krebs, M., Held, K., Binder, A., Hashimoto, K., Den Herder, G., Parniske, M., Kudla, J. and Schumacher, K. (2012). FRET-based genetically encoded sensors allow high-resolution live cell imaging of Ca(2)(+) dynamics. *Plant J.* **69**, 181-192.
Kriegel, A., Andrés, Z., Medzihradszky, A., Krüger, F., Scholl, S., Delang, S., Patir-Nebioglu, M. G., Gute, G., Yang, H., Murphy, A. S. et al. (2015). Job sharing in the endomembrane system: vacuolar acidification requires the combined activity of V-ATPase and V-PPase. *Plant Cell* **27**, 3383-3396.
Krzic, U., Gunther, S., Saunders, T. E., Streichan, S. J. and Hufnagel, L. (2012). Multiview light-sheet microscope for rapid in toto imaging. *Nat. Methods* **9**, 730-733.
Kuchitsu, K., Ward, J. M., Allen, G. J., Schelle, I. and Schroeder, J. I. (2002). Loading acetoxymethyl ester fluorescent dyes into the cytoplasm of Arabidopsis and Commelina guard cells. *New Phytol.* **153**, 527-533.
Kuner, T. and Augustine, G. J. (2000). A genetically encoded ratiometric indicator for chloride: capturing chloride transients in cultured hippocampal neurons. *Neuron* **27**, 447-459.
Kurihara, D., Mizuta, Y., Sato, Y. and Higashiyama, T. (2015). ClearSee: a rapid optical clearing reagent for whole-plant fluorescence imaging. *Development* **142**, 4168-4179.
Lager, I., Looger, L. L., Hilpert, M., Lalonde, S. and Frommer, W. B. (2006). Conversion of a putative Agrobacterium sugar-binding protein into a FRET sensor with high selectivity for sucrose. *J. Biol. Chem.* **281**, 30875-30883.
Lakowicz, J. R. (2006). *Principles of Fluorescence Spectroscopy*. Boston, MA: Springer Science+Business Media LLC.
Lanquar, V., Grossmann, G., Vinkenborg, J. L., Merkx, M., Thomine, S. and Frommer, W. B. (2014). Dynamic imaging of cytosolic zinc in Arabidopsis roots combining FRET sensors and RootChip technology. *New Phytol.* **202**, 198-208.
Laursen, T., Borch, J., Knudsen, C., Bavishi, K., Torta, F., Martens, H. J., Silvestro, D., Hatzakis, N. S., Wenk, M. R., Dafforn, T. R. et al. (2016). Characterization of a dynamic metabolon producing the defense compound dhurrin in sorghum. *Science* **354**, 890-893.
Legue, V., Blancaflor, E., Wymer, C., Perbal, G., Fantin, D. and Gilroy, S. (1997). Cytoplasmic free Ca2+ in Arabidopsis roots changes in response to touch but not gravity. *Plant Physiol.* **114**, 789-800.
Li, R., Liu, P., Wan, Y., Chen, T., Wang, Q., Mettbach, U., Baluska, F., Samaj, J., Fang, X., Lucas, W. J. et al. (2012). A membrane microdomain-associated protein, Arabidopsis Flot1, is involved in a clathrin-independent endocytic pathway and is required for seedling development. *Plant Cell* **24**, 2105-2122.
Long, Y., Stahl, Y., Weidtkamp-Peters, S., Postma, M., Zhou, W., Goedhart, J., Sánchez-Pérez, M.-I., Gadella, T. W. J., Simon, R., Scheres, B. et al. (2017). In vivo FRET-FLIM reveals cell-type-specific protein interactions in Arabidopsis roots. *Nature* **548**, 97-102.
Lorenzen, I., Aberle, T. and Plieth, C. (2004). Salt stress-induced chloride flux: a study using transgenic Arabidopsis expressing a fluorescent anion probe. *Plant J.* **38**, 539-544.
Lucas, M., Kenobi, K., von Wangenheim, D., Voss, U., Swarup, K., De Smet, I., Van Damme, D., Lawrence, T., Peret, B., Moscardi, E. et al. (2013). Lateral root morphogenesis is dependent on the mechanical properties of the overlaying tissues. *Proc. Natl. Acad. Sci. USA* **110**, 5229-5234.
Luo, Y., Scholl, S., Doering, A., Zhang, Y., Irani, N. G., Rubbo, S. D., Neumetzler, L., Krishnamoorthy, P., Van Houtte, I., Mylle, E. et al. (2015). V-ATPase activity in the TGN/EE is required for exocytosis and recycling in Arabidopsis. *Nat. Plants* **1**, 15094.
Maizel, A., von Wangenheim, D., Federici, F., Haseloff, J. and Stelzer, E. H. K. (2011). High-resolution live imaging of plant growth in near physiological bright conditions using light sheet fluorescence microscopy. *Plant J.* **68**, 377-385.
Martinière, A., Desbrosses, G., Sentenac, H. and Paris, N. (2013a). Development and properties of genetically encoded pH sensors in plants. *Front. Plant Sci.* **4**, 523.
Martinière, A., Bassil, E., Jublanc, E., Alcon, C., Reguera, M., Sentenac, H., Blumwald, E. and Paris, N. (2013b). In vivo intracellular pH measurements in tobacco and Arabidopsis reveal an unexpected pH gradient in the endomembrane system. *Plant Cell* **25**, 4028-4043.
Marty, L., Siala, W., Schwarzlander, M., Fricker, M. D., Wirtz, M., Sweetlove, L. J., Meyer, Y., Meyer, A. J., Reichheld, J.-P. and Hell, R. (2009). The NADPH-dependent thioredoxin system constitutes a functional backup for cytosolic glutathione reductase in Arabidopsis. *Proc. Natl. Acad. Sci. USA* **106**, 9109-9114.
Massalha, H., Korenblum, E., Malitsky, S., Shapiro, O. H. and Aharoni, A. (2017). Live imaging of root-bacteria interactions in a microfluidics setup. *Proc. Natl. Acad. Sci. USA* **114**, 4549-4554.
Mazzarello, P. (1999). A unifying concept: the history of cell theory. *Nat. Cell Biol.* **1**, E13-E15.
Meier, S. D., Kovalchuk, Y. and Rose, C. R. (2006). Properties of the new fluorescent Na+ indicator CoroNa Green: comparison with SBFI and confocal Na+ imaging. *J. Neurosci. Methods* **155**, 251-259.
Meier, M., Lucchetta, E. M. and Ismagilov, R. F. (2010). Chemical stimulation of the Arabidopsis thaliana root using multi-laminar flow on a microfluidic chip. *Lab. Chip* **10**, 2147-2153.
Miesenböck, G., De Angelis, D. A. and Rothman, J. E. (1998). Visualizing secretion and synaptic transmission with pH-sensitive green fluorescent proteins. *Nature* **394**, 192-195.
Minta, A. and Tsien, R. Y. (1989). Fluorescent indicators for cytosolic sodium. *J. Biol. Chem.* **264**, 19449-19457.
Miyawaki, A., Llopis, J., Heim, R., McCaffery, J. M., Adams, J. A., Ikura, M. and Tsien, R. Y. (1997). Fluorescent indicators for Ca2+ based on green fluorescent proteins and calmodulin. *Nature* **388**, 882-887.
Monshausen, G. B., Bibikova, T. N., Messerli, M. A., Shi, C. and Gilroy, S. (2007). Oscillations in extracellular pH and reactive oxygen species modulate tip growth of Arabidopsis root hairs. *Proc. Natl. Acad. Sci. USA* **104**, 20996-21001.
Monshausen, G. B., Bibikova, T. N., Weisenseel, M. H. and Gilroy, S. (2009). Ca2+ regulates reactive oxygen species production and pH during mechanosensing in Arabidopsis roots. *Plant Cell* **21**, 2341-2356.
Moseyko, N. and Feldman, L. J. (2001). Expression of pH-sensitive green fluorescent protein in Arabidopsis thaliana. *Plant Cell Environ.* **24**, 557-563.
Muday, G. K. (2001). Auxins and tropisms. *J. Plant Growth Regul.* **20**, 226-243.
Nagai, T., Yamada, S., Tominaga, T., Ichikawa, M. and Miyawaki, A. (2004). Expanded dynamic range of fluorescent indicators for Ca(2+) by circularly permuted yellow fluorescent proteins. *Proc. Natl. Acad. Sci. USA* **101**, 10554-10559.
Nezhad, A. S., Naghavi, M., Packirisamy, M., Bhat, R. and Geitmann, A. (2013). Quantification of the Young's modulus of the primary plant cell wall using Bending-Lab-On-Chip (BLOC). *Lab. Chip* **13**, 2599-2608.

Ngo, Q. A., Vogler, H., Lituiev, D. S., Nestorova, A. and Grossniklaus, U. (2014). A calcium dialog mediated by the FERONIA signal transduction pathway controls plant sperm delivery. *Dev. Cell* **29**, 491-500.
Oh, D.-H., Leidi, E., Zhang, Q., Hwang, S.-M., Li, Y., Quintero, F. J., Jiang, X., D'Urzo, M. P., Lee, S. Y., Zhao, Y. et al. (2009). Loss of halophytism by interference with SOS1 expression. *Plant Physiol.* **151**, 210-222.
Ortega-Villasante, C., Buren, S., Baron-Sola, A., Martinez, F. and Hernandez, L. E. (2016). *In vivo* ROS and redox potential fluorescent detection in plants: Present approaches and future perspectives. *Methods* **109**, 92-104.
Palmer, A. E., Giacomello, M., Kortemme, T., Hires, S. A., Lev-Ram, V., Baker, D. and Tsien, R. Y. (2006). Ca2+ indicators based on computationally redesigned calmodulin-peptide pairs. *Chem. Biol.* **13**, 521-530.
Parashar, A. and Pandey, S. (2011). Plant-in-chip: Microfluidic system for studying root growth and pathogenic interactions in Arabidopsis. *Appl. Phys. Lett.* **98**, 263703.
Park, M., Lee, H., Lee, J.-S., Byun, M.-O. and Kim, B.-G. (2009). In planta measurements of Na+ using fluorescent dye CoroNa green. *J. Plant Biol.* **52**, 298-302.
Poxson, D. J., Karady, M., Gabrielsson, R., Alkattan, A. Y., Gustavsson, A., Doyle, S. M., Robert, S., Ljung, K., Grebe, M., Simon, D. T. et al. (2017). Regulating plant physiology with organic electronics. *Proc. Natl. Acad. Sci. USA* **114**, 4597-4602.
Rayle, D. L. and Cleland, R. (1970). Enhancement of wall loosening and elongation by Acid solutions. *Plant Physiol.* **46**, 250-253.
Rellán-Álvarez, R., Lobet, G., Lindner, H., Pradier, P.-L., Sebastian, J., Yee, M.-C., Geng, Y., Trontin, C., LaRue, T., Schrager-Lavelle, A. et al. (2015). GLO-Roots: an imaging platform enabling multidimensional characterization of soil-grown root systems. *Elife* **4**, e07597.
Rink, T. J., Tsien, R. Y. and Pozzan, T. (1982). Cytoplasmic pH and free Mg2+ in lymphocytes. *J. Cell Biol.* **95**, 189-196.
Rizza, A., Walia, A., Lanquar, V., Frommer, W. B. and Jones, A. M. (2017). In vivo gibberellin gradients visualized in rapidly elongating tissues. *Nat. Plants* **3**, 803-813.
Rodrigues, O., Reshetnyak, G., Grondin, A., Saijo, Y., Leonhardt, N., Maurel, C. and Verdoucq, L. (2017). Aquaporins facilitate hydrogen peroxide entry into guard cells to mediate ABA- and pathogen-triggered stomatal closure. *Proc. Natl. Acad. Sci. USA* **114**, 9200-9205.
Rodriguez, A. A., Grunberg, K. A. and Taleisnik, E. L. (2002). Reactive oxygen species in the elongation zone of maize leaves are necessary for leaf extension. *Plant Physiol.* **129**, 1627-1632.
Sanford, L. and Palmer, A. (2017). Recent advances in development of genetically encoded fluorescent sensors. *Methods Enzymol.* **589**, 1-49.
Schopfer, P., Plachy, C. and Frahry, G. (2001). Release of reactive oxygen intermediates (superoxide radicals, hydrogen peroxide, and hydroxyl radicals) and peroxidase in germinating radish seeds controlled by light, gibberellin, and abscisic acid. *Plant Physiol.* **125**, 1591-1602.
Schubert, V. (2017). Super-resolution microscopy - applications in plant cell research. *Front. Plant Sci.* **8**, 531.
Schwarzländer, M., Fricker, M. D., Müller, C., Marty, L., Brach, T., Novak, J., Sweetlove, L. J., Hell, R. and Meyer, A. J. (2008). Confocal imaging of glutathione redox potential in living plant cells. *J. Microscopy.* **231**, 299-316.
Sena, G., Frentz, Z., Birnbaum, K. D. and Leibler, S. (2011). Quantitation of cellular dynamics in growing Arabidopsis roots with light sheet microscopy. *PLoS ONE* **6**, e21303.
Shaw, S. L. and Ehrhardt, D. W. (2013). Smaller, faster, brighter: advances in optical imaging of living plant cells. *Annu. Rev. Plant Biol.* **64**, 351-375.
Shen, J., Zeng, Y., Zhuang, X., Sun, L., Yao, X., Pimpl, P. and Jiang, L. (2013). Organelle pH in the Arabidopsis endomembrane system. *Mol Plant* **6**, 1419-1437.
Sia, S. K. and Whitesides, G. M. (2003). Microfluidic devices fabricated in poly (dimethylsiloxane) for biological studies. *Electrophoresis* **24**, 3563-3576.
Siemering, K. R., Golbik, R., Sever, R. and Haseloff, J. (1996). Mutations that suppress the thermosensitivity of green fluorescent protein. *Curr. Biol.* **6**, 1653-1663.
Sinclair, S. A., Sherson, S. M., Jarvis, R., Camakaris, J. and Cobbett, C. S. (2007). The use of the zinc-fluorophore, Zinpyr-1, in the study of zinc homeostasis in Arabidopsis roots. *New Phytol.* **174**, 39-45.
Slayman, C. L., Moussatos, V. V. and Webb, W. W. (1994). Endosomal accumulation of pH indicator dyes delivered as acetoxymethyl esters. *J. Exp. Biol.* **196**, 419-438.
Somssich, M., Ma, Q., Weidtkamp-Peters, S., Stahl, Y., Felekyan, S., Bleckmann, A., Seidel, C. A. M. and Simon, R. (2015). Real-time dynamics of peptide ligand-dependent receptor complex formation in planta. *Sci. Signal.* **8**, ra76.
Song, W.-Y., Choi, K. S., Kim, D. Y., Geisler, M., Park, J., Vincenzetti, V., Schellenberg, M., Kim, S. H., Lim, Y. P., Noh, E. W. et al. (2010). Arabidopsis PCR2 is a zinc exporter involved in both zinc extrusion and long-distance zinc transport. *Plant Cell* **22**, 2237-2252.
Stahl, Y., Grabowski, S., Bleckmann, A., Kühnemuth, R., Weidtkamp-Peters, S., Pinto, K. G., Kirschner, G. K., Schmid, J. B., Wink, R. H., Hülsewede, A. et al. (2013). Moderation of Arabidopsis root stemness by CLAVATA1 and ARABIDOPSIS CRINKLY4 receptor kinase complexes. *Curr. Biol.* **23**, 362-371.
Stanley, C. E. and van der Heijden, M. G. A. (2017). Microbiome-on-a-Chip: new frontiers in plant-microbiota research. *Trends Microbiol.* **25**, 610-613.
Stanley, C. E., Grossmann, G., Casadevall i Solvas, X. and deMello, A. J. (2016). Soil-on-a-Chip: microfluidic platforms for environmental organismal studies. *Lab. Chip* **16**, 228-241.
Stanley, C. E., Shrivastava, J., Brugman, R., Heinzelmann, E., van Swaay, D. and Grossmann, G. (2017). Dual-flow-RootChip reveals local adaptations of roots towards environmental asymmetry at the physiological and genetic levels. *New Phytol.*, doi:10.1111/nph.14887.
Stelzer, E. H. K. (2015). Light-sheet fluorescence microscopy for quantitative biology. *Nat. Methods* **12**, 23-26.
Swanson, S. J., Choi, W. G., Chanoca, A. and Gilroy, S. (2011). *In vivo* imaging of Ca2+, pH, and reactive oxygen species using fluorescent probes in plants. *Annu. Rev. Plant Biol.* **62**, 273-297.
Swanson, S. J. and Jones, R. L. (1996). Gibberellic acid induces vacuolar acidification in barley aleurone. *Plant Cell* **8**, 2211-2221.
Tantama, M., Martínez-François, J. R., Mongeon, R. and Yellen, G. (2013). Imaging energy status in live cells with a fluorescent biosensor of the intracellular ATP-to-ADP ratio. *Nat. Commun.* **4**, 2550.
Thestrup, T., Litzlbauer, J., Bartholomäus, I., Mues, M., Russo, L., Dana, H., Kovalchuk, Y., Liang, Y., Kalamakis, G., Laukat, Y. et al. (2014). Optimized ratiometric calcium sensors for functional in vivo imaging of neurons and T lymphocytes. *Nat. Methods* **11**, 175-182.
Tian, L., Hires, S. A., Mao, T., Huber, D., Chiappe, M. E., Chalasani, S. H., Petreanu, L., Akerboom, J., McKinney, S. A., Schreiter, E. R. et al. (2009). Imaging neural activity in worms, flies and mice with improved GCaMP calcium indicators. *Nat. Methods* **6**, 875-881.
Ueno, T. and Nagano, T. (2011). Fluorescent probes for sensing and imaging. *Nat. Methods* **8**, 642-645.
Uslu, V. V. and Grossmann, G. (2016). The biosensor toolbox for plant developmental biology. *Curr. Opin. Plant Biol.* **29**, 138-147.
Ustione, A. and Piston, D. W. (2011). A simple introduction to multiphoton microscopy. *J. Microsc.* **243**, 221-226.
Vincent, T. R., Avramova, M., Canham, J., Higgins, P., Bilkey, N., Mugford, S. T., Pitino, M., Toyota, M., Gilroy, S., Miller, A. J. et al. (2017). Interplay of plasma membrane and vacuolar ion channels, together with BAK1, elicits rapid cytosolic calcium elevations in arabidopsis during aphid feeding. *Plant Cell* **29**, 1460-1479.
Vinkenborg, J. L., Nicolson, T. J., Bellomo, E. A., Koay, M. S., Rutter, G. A. and Merkx, M. (2009). Genetically encoded FRET sensors to monitor intracellular Zn2+ homeostasis. *Nat. Methods* **6**, 737-740.
Viotti, C., Kruger, F., Krebs, M., Neubert, C., Fink, F., Lupanga, U., Scheuring, D., Boutte, Y., Frescatada-Rosa, M., Wolfenstetter, S. et al. (2013). The endoplasmic reticulum is the main membrane source for biogenesis of the lytic vacuole in Arabidopsis. *Plant Cell* **25**, 3434-3449.
von Wangenheim, D., Fangerau, J., Schmitz, A., Smith, R. S., Leitte, H., Stelzer, E. H. K. and Maizel, A. (2016). Rules and self-organizing properties of post-embryonic plant organ cell division patterns. *Curr. Biol.* **26**, 439-449.
von Wangenheim, D., Hauschild, R., Fendrych, M., Barone, V., Benková, E. and Friml, J. (2017). Live tracking of moving samples in confocal microscopy for vertically grown roots. *Elife* **6**, e26792.
Waadt, R., Hitomi, K., Nishimura, N., Hitomi, C., Adams, S. R., Getzoff, E. D. and Schroeder, J. I. (2014). FRET-based reporters for the direct visualization of abscisic acid concentration changes and distribution in Arabidopsis. *Elife* **3**, e01739.
Waadt, R., Krebs, M., Kudla, J. and Schumacher, K. (2017). Multiparameter imaging of calcium and abscisic acid and high-resolution quantitative calcium measurements using R-GECO1-mTurquoise in Arabidopsis. *New Phytol.* **216**, 303-320.
Wagner, S., Behera, S., De Bortoli, S., Logan, D. C., Fuchs, P., Carraretto, L., Teardo, E., Cendron, L., Nietzel, T., Fussl, M. et al. (2015). The EF-Hand Ca2+ binding protein MICU choreographs mitochondrial Ca2+ dynamics in arabidopsis. *Plant Cell* **27**, 3190-3212.
Walkup, G. K., Burdette, S. C., Lippard, S. J. and Tsien, R. Y. (2000). A new cell-permeable fluorescent probe for Zn2+. *J. Am. Chem. Soc.* **122**, 5644-5645.
Wan, Y., Ash, W. M., III, Fan, L., Hao, H., Kim, M. K. and Lin, J. (2011). Variable-angle total internal reflection fluorescence microscopy of intact cells of Arabidopsis thaliana. *Plant Methods* **7**, 27.
Wang, L., Li, H., Lv, X., Chen, T., Li, R., Xue, Y., Jiang, J., Jin, B., Baluška, F., Šamaj, J. et al. (2015a). Spatiotemporal dynamics of the BRI1 receptor and its regulation by membrane microdomains in living arabidopsis cells. *Mol. Plant* **8**, 1334-1349.
Wang, X., Li, X., Deng, X., Luu, D.-T., Maurel, C. and Lin, J. (2015b). Single-molecule fluorescence imaging to quantify membrane protein dynamics and oligomerization in living plant cells. *Nat. Protoc.* **10**, 2054-2063.

Weidtkamp-Peters, S. and Stahl, Y. (2017). The use of FRET/FLIM to study proteins interacting with plant receptor kinases. *Methods Mol. Biol.* **1621**, 163-175.

Weidtkamp-Peters, S., Felekyan, S., Bleckmann, A., Simon, R., Becker, W., Kühnemuth, R. and Seidel, C. A. M. (2009). Multiparameter fluorescence image spectroscopy to study molecular interactions. *Photochem. Photobiol. Sci.* **8**, 470-480.

Whitesides, G. M. (2006). The origins and the future of microfluidics. *Nature* **442**, 368-373.

Xing, S., Mehlhorn, D. G., Wallmeroth, N., Asseck, L. Y., Kar, R., Voss, A., Denninger, P., Schmidt, V. A. F., Schwarzländer, M., Stierhof, Y.-D. et al. (2017). Loss of GET pathway orthologs in Arabidopsis thaliana causes root hair growth defects and affects SNARE abundance. *Proc. Natl. Acad. Sci. USA* **114**, E1544-E1553.

Yanagisawa, N., Sugimoto, N., Arata, H., Higashiyama, T. and Sato, Y. (2017). Capability of tip-growing plant cells to penetrate into extremely narrow gaps. *Sci. Rep.* **7**, 1403.

Yang, H., Bogner, M., Stierhof, Y.-D. and Ludewig, U. (2010). H+-independent glutamine transport in plant root tips. *PLoS ONE* **5**, e8917.

Zhao, Y., Araki, S., Wu, J., Teramoto, T., Chang, Y.-F., Nakano, M., Abdelfattah, A. S., Fujiwara, M., Ishihara, T., Nagai, T. et al. (2011). An expanded palette of genetically encoded Ca(2)(+) indicators. *Science* **333**, 1888-1891.

Zheng, W., Wu, Y., Winter, P., Fischer, R., Nogare, D. D., Hong, A., McCormick, C., Christensen, R., Dempsey, W. P., Arnold, D. B. et al. (2017). Adaptive optics improves multiphoton super-resolution imaging. *Nat. Methods* **14**, 869-872.

Zhujun, Z. and Seitz, W. R. (1984). A carbon dioxide sensor based on fluorescence. *Anal. Chim. Acta* **160**, 305-309.